PLATE BENDING FINITE ELEMENT ANALYSIS OF BEAMS WITH WEB OPENINGS

by

HSIANG-HUAN LEE

Diploma, Taipei Institute of Technology,
Taiwan, China, 1965

9984

A MASTER'S REPORT

submitted in partial fulfillment of the

requirements for the degree

MASTER OF SCIENCE

Department of Civil Engineering

KANSAS STATE UNIVERSITY
Manhattan, Kansas

1972

Approved by:

Robert L. Lee

Major Professor

LD
2668
R4
1972
M45
COPY 2

TABLE OF CONTENTS

INTRODUCTION

1. Introduction

In the present construction of steel buildings, openings through the webs of steel beams are frequently necessary to accommodate the passage of pipes, ducts and other utility components. Thus, the strength of the beam may be weakened to the extent that reinforcing is required in the vicinity of the openings. In the past few years, both analytical and experimental investigations have been made of the stresses around various openings with and without reinforcing. Several theoretical solutions have been verified and are available for certain cases of this problem. The purpose of this study was to determine the accuracy of an analytical solution based on a 'Finite Element Method' by comparing these results with those of an experimental program carried out at Kansas State University(1)*. The results were also compared with the results obtained using a Vierendeel Analysis (1).

An A36 W12x45 steel beam with a 6" x 9" rectangular web opening at middepth, subjected to combined bending and shear, was treated as a three dimensional plate structure in this study. The finite element method was used to investigate the stress distribution around the rectangular hole. An existing computer program (2) was made operational as a requirement of this report.

---

*Numbers in parentheses refer to corresponding items in the " References ".

2. Objectives

The primary objectives of this report were:

a. To obtain a solution to the problem using the finite element method.

b. To compare the results of this study with the experimental results and with predictions based on the so-called Vierendeel Method of analysis (1).

3. Scope

The study was limited to A36 steel W12x45 shapes with a 6" x 9" rectangular web opening centered on the neutral axis of the beams, which were subjected to combined bending and shear with various values of the moment-shear ratio obtained by placing a given concentrated load at the center of the span and simultaneously varying the shear span length. Both reinforced and unreinforced openings were studied. The reinforcing consisted of horizontal bars located above and below the opening, on just one side of the web.

LITERATURE REVIEW

In 1932, Muskhelishvili introduced the application of the comformal mapping technique and complex integration to the problems of plane elasticity (3).

In 1958, Heller, Brock and Bart presented a solution by the complex variable method associated with Muskhelishvili for the stresses around a rectangular opening with rounded corners in a uniformly loaded plate (4). In 1962, they used the same method to investigate the stresses around a rectangular opening with rounded corners in a beam subjected to bending and shear (5). In both cases, they reached the conclusion that the maximum value of the boundary stress is a function of both aspect ratio (height-to-width) and corner radius.

Snell, in 1962, used the finite element method to study the effects of various reinforcing configurations for rectangular openings in plates subjected to uniaxial tension (6). After his analytical and experimental studies, he reached the following conclusions: (a) The finite element method could be used for the solution of this type of problem. (b) Reinforcing strips parallel to the direction of the applied load could effectively be used to reduce stress concentration in plates with rectangular openings. (c) The most effective length for these strips was closely approximated by placing the reinforcing in such a way that the ends were on lines drawn outward from the corners of the opening in the plate at 45° angle to the plate axes.

In 1964, Segner made a study of the reinforcing requirements around large rectangular web openings in W shape beams subjected to varying combinations of bending moment and shear (7). His theoretical approach was based on the theory that a member having such openings centered on the neutral axis acts as a Vierendeel truss and thus has a point of contraflexure at mid-length of each opening above and below the opening in the tee section. After his experimental study, he concluded that the Vierendeel theory was an appropriate analogy for this problem. Since then, the so-called 'Vierendeel Method' has frequently been used by designers to calculate the elastic stresses around rectangular holes in the web of W shape beams.

Bower developed an analytical method, in 1966, also using the complex stress function to predict the elastic stresses around elliptic and circular holes in the webs of W shape beams under a uniform load. The applicability of this analysis depends on the size and shape of the web hole and on the magnitude of the moment-shear ratio at the center of the hole (8). In the same year, he conducted tests on simply supported W shape beams with circular or rectangular web openings loaded by concentrated loads (9). He concluded that for circular and rectangular holes the elastic analysis could accurately predict the tangential stress along the hole and the bending stress on transverse cross sections in the vicinity of the hole, when the hole did not exceed half of the web depth. He also concluded that the Vierendeel analysis predicts a reasonably accurate bending stress

except for local stress concentrations at the hole corners.

In 1969, Cheng experimentally analyzed the stresses around a rectangular web opening in a W shape beam using the photostress method and electrical resistance strain gage techniques (10). One of his conclusions was that simple beam theory could not be used to predict normal stress within the region on either side of the opening for a distance approximately equal to the depth of the beam. In this region the normal bending stress distribution is non-linear.

METHOD OF ANALYSIS

1. Introduction

The concept of the finite element method was originally introduced by Turner et al. in 1956 (11). O. C. Zienkiewicz and Y. K. Cheng (12) also presented the theory necessary for the analysis of a plane elastic continua. By using this method a plane elastic continua is divided into elements interconnected at a finite number of nodes. When the force-displacement relationships for the individual elements are determined, the general 'displacement method' of structural analysis procedure can be conveniently followed.

In this report, the W shape beam is treated as a three-dimensional structure. The elements then may be subjected to both bending and 'in plane' forces. For a flat element these leadings cause independent deformations, and the stiffness matrix for plane stress and plate bending can each be determined separately..The total element stiffness matrix can then be made up by simply combining these two matrices. Flat triangular elements are used with constant strain properties for the plane stress components, and linear strain variation for bending. For bending, a non-comforming shape function is used. The matrix formulation of the finite element analysis as presented in Reference (12) is included here for the purpose of providing some insight into the method.

2. Formulation of the General Equations

The general displacement method equation is given (13) as

$$\{F\}^e = [K]^e\{\delta\}^e \tag{1}$$

in which

$\{F\}^e$ = column matrix of nodal forces for a particular element (in local coordinates),

$[K]^e$ = element stiffness matrix (in local coordinates), and

$\{\delta\}^e$ = column matrix of nodal displacements for a particular element (in local coordinates).

Internal displacements are expressed in terms of the nodal displacements by

$$\{f\} = [N]\{\delta\}^e \tag{2}$$

in which

$\{f\}$ = column matrix of internal displacements in the element, and

$[N]$ = square matrix dependent upon the element geometry, relating the internal displacements and nodal displacements.

The strains at any point within the element can be determined by

$$\{\epsilon\} = [B]\{\delta\}^e \tag{3}$$

in which

$\{\epsilon\}$ = the column matrix of total strains at any point within the element, and

$[B]$ = square matrix obatined from the appropriate

strain-displacement relationships governing the element.

The relationship between stress and strain can be written as

$$\{\sigma\} = [D]\{\epsilon\} \tag{4}$$

in which

$\{\sigma\}$ = column matrix of stresses within the element, and

$[D]$ = square matrix of material constants relating internal stress to strain.

Substituting from equation (3) into equation (4) yields

$$\{\sigma\} = [D][B]\{\delta\}^e. \tag{5}$$

The element stiffness matrix can now be derived by using an energy method (15). The total strain energy of the element is

$$U = \frac{1}{2}\int_V \{\epsilon\}^T\{\sigma\}\,dv. \tag{6}$$

Substituting from equations (3) and (5) into (6) yields

$$U = \frac{1}{2}\int_V (\{\delta\}^e)^T [B]^T [D][B]\{\delta\}^e\,dv. \tag{7}$$

The average work done by the nodal forces is

$$W = \frac{1}{2}(\{F\}^e)^T\{\delta\}^e. \tag{8}$$

Substituting from equation (1) into equation (8) yields

$$W = \frac{1}{2}(\{\delta\}^e)^T [K]^e\{\delta\}^e. \tag{9}$$

Since the external work W must equal the energy, U, absorbed by the element, a comparison of equations (7) and (9)

reveals that

$$[K]^e = \int_v [B]^T [D] [B] \, dv. \tag{10}$$

The element stiffness matrix in local coordinates must be transformed into the global coordinate system in order to assemble the elements. Let

$$\{\delta\}^e = [T] \{\bar{\delta}\}^e \quad \text{and} \quad \{F\}^e = [T] \{\bar{F}\}^e \tag{11}$$

in which

$[T]$ = transformation matrix,

$\{\bar{\delta}\}^e$ = column matrix of nodal displacements for a particular element (in global coordinates), and

$\{\bar{F}\}^e$ = column matrix of nodal forces for a particular element (in global coordinates).

Substituting from equation (11) into equation (1) yields

$$\{\bar{F}\}^e = [T]^T [K]^e [T] \{\bar{\delta}\}^e. \tag{12}$$

The stiffness matrix of an element in the global coordinates then becomes

$$[\bar{K}]^e = [T]^T [K]^e [T]. \tag{13}$$

When the overall equilibrium conditions are established at the nodes of the structure, the resulting equations will contain the displacements as unknowns. Once these have been solved, the stresses can be found by using equation (5) for each element, in turn.

3. Triangular Plate Element

a. Plate in Plane Stress

Let a typical triangular plate element with nodes i, j and m noted in a counter-clockwise order be as shown in

Fig. 1. The plane displacements of a node each have two components

$$\{\delta_i\} = \begin{Bmatrix} u_i \\ v_i \end{Bmatrix} . \tag{14}$$

The six components of element displacements can then be listed as a column vector.

$$\{\delta\}^e = \begin{Bmatrix} \delta_i \\ \delta_j \\ \delta_m \end{Bmatrix} \tag{15}$$

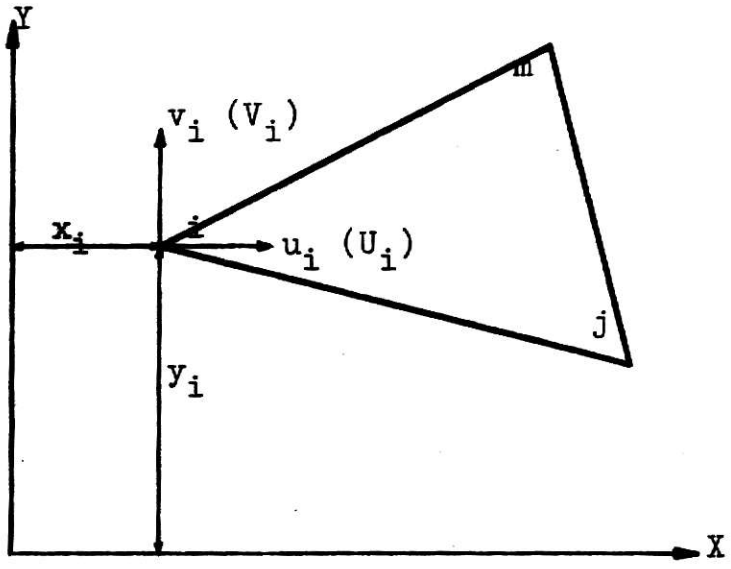

Fig. 1 Triangular Plate Plane Stress Element

The displacements at any point within an element are defined by these six values as

$$\{f\} = \begin{Bmatrix} u(x,y) \\ v(x,y) \end{Bmatrix} = [N]\{\delta\}^e \tag{16}$$

in which u and v are the internal displacements in the x and y directions, respectively. Two linear polynomials

$$u = \alpha_1 + \alpha_2 x + \alpha_3 y, \text{ and}$$
$$v = \alpha_4 + \alpha_5 x + \alpha_6 y \tag{17}$$

are chosen to represent the displacement field for the element. On substituting the boundary conditions

$$u = u_i \quad \text{and} \quad v = v_i \quad \text{at} \quad (x_i, y_i),$$
$$u = u_j \quad \text{and} \quad v = v_j \quad \text{at} \quad (x_j, y_j), \tag{18}$$
$$\text{and} \quad u = u_m \quad \text{and} \quad v = v_m \quad \text{at} \quad (x_m, y_m)$$

into equation (17), the six undetermined coefficients can be determined. For example,

$$u_i = \alpha_1 + \alpha_2 x_i + \alpha_3 y_i,$$
$$u_j = \alpha_1 + \alpha_2 x_j + \alpha_3 y_j, \text{ and} \tag{19}$$
$$u_m = \alpha_1 + \alpha_2 x_m + \alpha_3 y_m.$$

We can solve for α_1, α_2 and α_3 in terms of the nodal displacements u_i, u_j and u_m. In the same way α_4, α_5 and α_6 can be obtained. We finally find that

$$u = \frac{1}{2\Delta}[(a_i+b_i x+c_i y)u_i+(a_j+b_j x+c_j y)u_j+(a_m+b_m x+c_m y)u_m], \text{and}$$
$$v = \frac{1}{2\Delta}[(a_i+b_i x+c_i y)v_i+(a_j+b_j x+c_j y)v_j+(a_m+b_m x+c_m y)v_m] \tag{20}$$

in which

$$a_i = x_j y_m - x_m y_j,$$
$$b_i = y_j - y_m = y_{jm},$$
$$c_i = x_m - x_j = x_{mj},$$

$$
\begin{aligned}
a_j &= x_m y_i - x_i y_m, \\
b_j &= y_m - y_i = y_{mi}, \\
c_j &= x_i - x_m = x_{im}, \\
a_m &= x_i y_j - x_j y_i, \\
b_m &= y_i - y_j = y_{ij}, \text{ and} \\
c_m &= x_j - x_i = x_{ji}
\end{aligned} \tag{21}
$$

and where

$$
2\Delta = \det \begin{vmatrix} 1 & x_i & y_i \\ 1 & x_j & y_j \\ 1 & x_m & y_m \end{vmatrix} = 2 \text{ (area of triangle i, j, m)}. \tag{22}
$$

We can represent the relations in equation (20) in the form of equation (16)

$$
\{f\} = \begin{Bmatrix} u \\ v \end{Bmatrix} = [N]\{\delta\}^e = [\, IN_i', IN_j', IN_m' \,]\{\delta\}^e \tag{23}
$$

where I is a two by two identity matrix and

$$
\begin{aligned}
N_i' &= \frac{(a_i + b_i x + c_i y)}{2\Delta}, \\
N_j' &= \frac{(a_j + b_j x + c_j y)}{2\Delta}, \text{ and} \\
N_m' &= \frac{(a_m + b_m x + c_m y)}{2\Delta}.
\end{aligned} \tag{24}
$$

The calculation of the coefficients can be simplified if the reference coordinates are taken as the centroid of the element. When that is done, the relationships

$$x_i+x_j+x_m = y_i+y_j+y_m$$

and $$a_i = \frac{2\Delta}{3} = a_j = a_m \tag{25}$$

result.

The total strain at any point within the element can be defined in terms of the displacements by well-known (14) relationships

$$\{\epsilon\} = \begin{Bmatrix} \epsilon_x \\ \epsilon_y \\ \epsilon_{xy} \end{Bmatrix} = \begin{Bmatrix} \frac{\partial u}{\partial x} \\ \frac{\partial v}{\partial y} \\ \frac{\partial u}{\partial y} + \frac{\partial v}{\partial x} \end{Bmatrix} . \tag{26}$$

Taking the appropriate partial derivatives of equation (20), results in

$$\{\epsilon\} = \frac{1}{2\Delta} \begin{bmatrix} b_i, & 0, & b_j, & 0, & b_m, & 0 \\ 0, & c_i, & 0, & c_j, & 0, & c_m \\ c_i, & b_i, & c_j, & b_j, & c_m, & b_m \end{bmatrix} \{\delta\}^e \tag{27}$$

or, to correspond with equation (3)

$$\{\epsilon\} = [B]\{\delta\}^e$$

where

$$[B] = \frac{1}{2\Delta}\begin{bmatrix} b_i, & 0, & b_j, & 0, & b_m, & 0 \\ 0, & c_i, & 0, & c_j, & 0, & c_m \\ c_i, & b_i, & c_j, & b_j, & c_m, & b_m \end{bmatrix} . \tag{28}$$

The relationship between stress and strain is defined by equation (4). For the plane stress case, three components of stress correspond to the strains already defined as

$$\{\sigma\} = \begin{Bmatrix} \sigma_x \\ \sigma_y \\ \tau_{xy} \end{Bmatrix} . \tag{29}$$

For a linearly elastic, homogeneous and isotropic material, the matrix of material constants for this case is obtained from Hooke's law as

$$[D] = \frac{E}{1-\mu^2}\begin{bmatrix} 1 & \mu & 0 \\ \mu & 1 & 0 \\ 0 & 0 & (1-\mu)/2 \end{bmatrix} . \tag{30}$$

For the plane strain case, a similar matrix can be formed.

The stiffness matrix of the element i, j, m is defined by the relationship in equation (10) as

$$[K]^e = \int_v [B]^T [D] [B] \, t \, dx \, dy \tag{31}$$

where t is the constant thickness of the element and the integration is taken over the area of the triangular element.

Since neither of the matrices in equation (31) contains x nor y, we have

$$[K]^e = [B]^T [D] [B] t \Delta \tag{32}$$

where Δ is the area of the triangle as defined by equation (22).

b. Plate Bending Stress

Consider a triangular plate i, j, m coinciding with the x, y plane as shown in Fig. 2. At each node, displacements $\{\delta_n\}$ are introduced. These have three components: the first a deflection w_n in the Z-direction, the second a rotation $(\theta_x)_n$ about the X-axis through the node and the third a rotation $(\theta_y)_n$ about the Y-axis through the node.

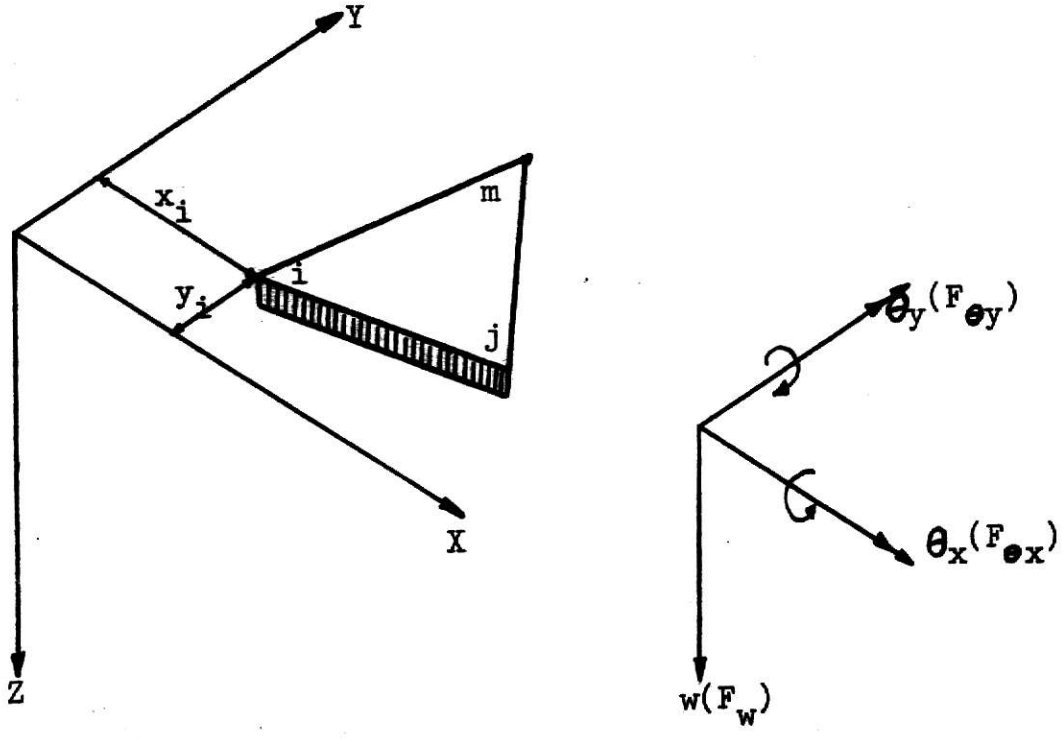

Fig. 2 Triangular Plate Element in Bending

The positive directions of the rotations are determined by the right-hand screw rule and are shown as vectors directed along the axes. The three components of nodal displacement at a node i can therefore be defined (16) as follows:

$$\{\delta_i\} = \begin{Bmatrix} w_i \\ \theta_{xi} \\ \theta_{yi} \end{Bmatrix} = \begin{Bmatrix} w_i \\ -(\frac{\partial w}{\partial y})_i \\ (\frac{\partial w}{\partial x})_i \end{Bmatrix} \tag{33}$$

and the corresponding force vector

$$\{F_i\} = \begin{Bmatrix} (F_w)_i \\ (F_{\theta x})_i \\ (F_{\theta y})_i \end{Bmatrix}. \tag{34}$$

The shape functions now must be definable in terms of $\{\delta\}^e$, that is in terms of nine parameters. A polynomial expression is conveniently used. We can write

$$w = f(x,y) = \alpha_1+\alpha_2 x+\alpha_3 y+\alpha_4 x^2+\alpha_5 xy+\alpha_6 y^2+\alpha_7 x^3+\alpha_8(px^2y+qxy^2) +\alpha_9 y^3 . \tag{35}$$

The undetermined coefficients α_1 to α_9 can be evaluated by writing the nine simultaneous equations linking the values of w and its slopes at the nodes when the coordinates take up their appropriate values. For instance

$$w_i = \alpha_1+\alpha_2 x_i+\alpha_3 y_i+\alpha_4 x_i^2+\alpha_5 x_i y_i+\alpha_6 y_i^2+\alpha_7 x_i^3 +\alpha_8(px_i^2 y_i+qx_i y_i^2)+\alpha_9 y_i^3,$$

$$\left(\frac{-\partial w}{\partial y}\right)_i = -\alpha_3 - \alpha_5 y_i - 2\alpha_6 y_i - \alpha_8 (p x_i^2 + 2q x_i y_i) - 3\alpha_9 y_i^2 \text{ , and} \quad (36)$$

$$\left(\frac{\partial w}{\partial x}\right)_i = \alpha_2 + 2\alpha_4 x_i + \alpha_5 y_i + 3\alpha_7 x_i^2 + \alpha_8 (2p x_i y_i + q y_i^2).$$

We can write all nine equations in matrix form,

$$\{\delta\}^e = [C]\{\alpha\} \quad (37)$$

where [C] is a nine by nine matrix depending on nodal coordinates and $\{\alpha\}$ a vector of the nine undetermined coefficients. Inverting [C] and solving for $\{\alpha\}$ yields

$$\{\alpha\} = [C]^{-1}\{\delta\}^e. \quad (38)$$

It is now possible to write the expression for the displacement within the element in the form of equation (2)

$$\{f\} = w = [N]\{\delta\}^e = [P]\,[C]^{-1}\{\delta\}^e \quad (39)$$

where

$$[P] = (1,\ x,\ y,\ x^2,\ xy,\ y^2,\ x^3, px^2y + qxy^2,\ y^3), \quad (40)$$

and

$p = q = 1$, for Tochers function (2), or

$p = 0,\ q = 1$, for Gallaghers function (2).

According to classical plate theory (16), for any point in a plate, the generalized 'strain' can be defined as

$$\{\epsilon\} = \begin{Bmatrix} -\dfrac{\partial^2 w}{\partial x^2} \\ -\dfrac{\partial^2 w}{\partial y^2} \\ 2\dfrac{\partial^2 w}{\partial x \partial y} \end{Bmatrix} \quad (41)$$

and the corresponding generalized 'stress' as

$$\{\sigma\} = \{M\} = \begin{Bmatrix} M_x \\ M_y \\ M_{xy} \end{Bmatrix} \tag{42}$$

with the notation and positive directions as shown in Fig. 3. The actual stresses are determined by such expressions as

$$\sigma_x = \frac{6M_x}{t^2},$$

$$\sigma_y = \frac{6M_y}{t^2}, \text{ and} \tag{43}$$

$$\tau_{xy} = \frac{6M_{xy}}{t^2}.$$

Equation (41) can also be written in the form of equation (3)

$$\{\epsilon\} = [B]\{\delta\}^e. \tag{3}$$

The vector, $\{\epsilon\}$, can be obtained directly from equation (35), as

$$\{\epsilon\} = \begin{Bmatrix} (-2\alpha_4 & -6\alpha_7 x & -2p\alpha_8 y) \\ (-2\alpha_6 & -2q\alpha_8 x & -6\alpha_9 y) \\ (2\alpha_5 & 4(px+qy)\alpha_8 &) \end{Bmatrix} \tag{44}$$

which can be written as

$$\{\epsilon\} = [Q]\{\alpha\} = [Q]\,[C]^{-1}\{\delta\}^e \tag{45}$$

and thus

$$[B] = [Q]\,[C]^{-1} \tag{46}$$

in which

$$[Q] = \begin{bmatrix} 0, & 0, & 0, & -2, & 0, & 0, & -6x, & -2py, & 0 \\ 0, & 0, & 0, & 0, & 0, & -2, & 0, & -2x, & -6y \\ 0, & 0, & 0, & 0, & 2, & 0, & 0, & 4(px+qy), & 0 \end{bmatrix}. \quad (47)$$

The linear relationship between stress and strain is derived as

$$\{\sigma\} = \{M\} = [D]\{\epsilon\}. \quad (48)$$

For an isotropic plate

$$[D] = \frac{Et^3}{12(1-\mu^2)} \begin{bmatrix} 1 & \mu & 0 \\ \mu & 1 & 0 \\ 0 & 0 & (1-\mu)/2 \end{bmatrix}. \quad (49)$$

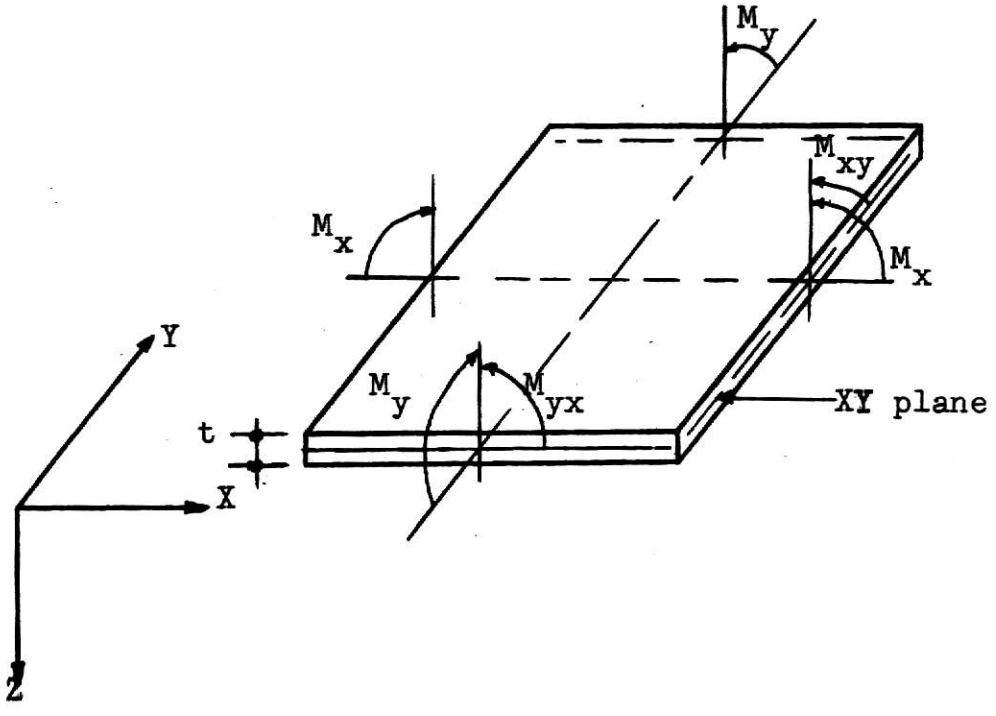

Fig. 3 Stress Resultants of 'Stresses' in Plate Bending

The stiffness matrix can now, again, be developed by an energy method as indicated in equation (10)

$$[K] = \iint [B]^T [D] [B] \, dx \, dy \, . \tag{50}$$

Substituting equation (46) and taking t as a constant within the element, yields

$$[K] = \left\{ [C]^{-1} \right\}^T \left(\iint [Q]^T [D] [Q] \, dx \, dy \right) [C]^{-1} . \tag{51}$$

c. Combining 'In Plane' And Bending Actions

From the previous derivations, we obtain the stiffness matrix and the relationships

$$\begin{Bmatrix} F_i^p \\ F_j^p \\ F_m^p \end{Bmatrix} = [K]^p \begin{Bmatrix} \delta_i^p \\ \delta_j^p \\ \delta_m^p \end{Bmatrix}$$

with $\left\{ \delta_i^p \right\} = \begin{Bmatrix} u_i \\ v_i \end{Bmatrix}$ and $\left\{ F_i^p \right\} = \begin{Bmatrix} U_i \\ V_i \end{Bmatrix}$ (52)

for in plane (Plane stress) action,

and

$$\begin{Bmatrix} F_i^b \\ F_j^b \\ F_m^b \end{Bmatrix} = [K]^b \begin{Bmatrix} \delta_i^b \\ \delta_j^b \\ \delta_m^b \end{Bmatrix}$$

with

$$\left\{\delta_i^b\right\} = \begin{Bmatrix} w_i \\ \theta_{xi} \\ \theta_{yi} \end{Bmatrix} \quad \text{and} \quad \left\{F_i^b\right\} = \begin{Bmatrix} F_{wi} \\ F_{\theta xi} \\ F_{\theta yi} \end{Bmatrix} \tag{53}$$

for plate bending action.

Before combining these stiffnesses it is important to note two facts. The first is that the displacements prescribed for 'in plane' forces do not affect the bending deformations and vice versa. The second is that rotation θ_z does not enter as a parameter into the definition of deformations in either mode. It is convenient to take this rotation into account and associate with it a fictious couple $F_{\theta z}$. It is also necessary to insert an appropriate number of zeros into the stiffness matrices. Redefining, now, the combined nodal displacements as

$$\left\{\delta_i\right\} = \begin{Bmatrix} u_i \\ v_i \\ w_i \\ \theta_{xi} \\ \theta_{yi} \\ \theta_{zi} \end{Bmatrix} \tag{54}$$

and the corresponding 'forces' as

$$\left\{ F_i \right\} = \begin{Bmatrix} U_i \\ V_i \\ F_{wi} \\ F_{\theta xi} \\ F_{\theta yi} \\ F_{\theta zi} \end{Bmatrix} , \tag{55}$$

we can write

$$\begin{Bmatrix} F_i \\ F_j \\ F_m \end{Bmatrix} = [K]^e \begin{Bmatrix} \delta_i \\ \delta_j \\ \delta_m \end{Bmatrix} \tag{56}$$

or in the form of equation (1)

$$\left\{ F \right\}^e = [K]^e \left\{ \delta \right\}^e . \tag{1}$$

d. Transformation to Global Coordinates

The previous derivations of stiffness matrices are based on local coordinates. Transformation of coordinates to a common global system (which is denoted by $\bar{x}$, $\bar{y}$, $\bar{z}$, while the local system is denoted by x, y, z, as shown in Fig. 4) will be necessary in order to assemble the elements and write the appropriate equilibrium equations.

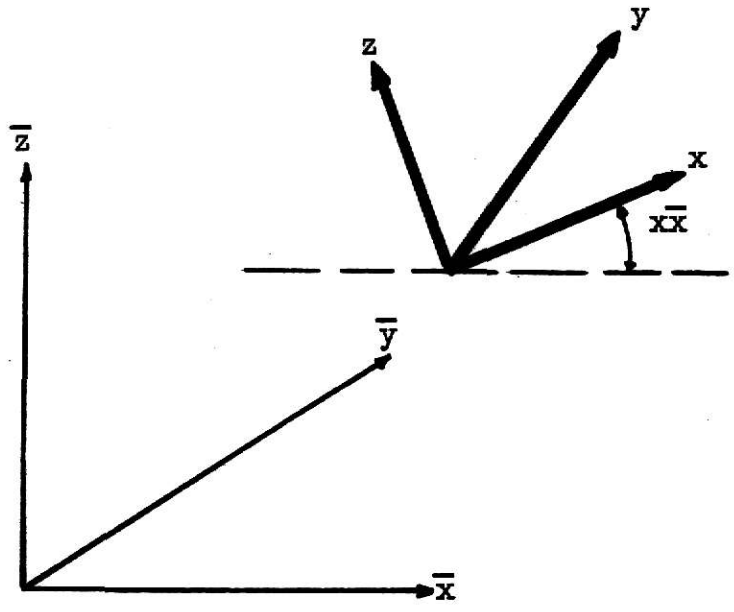

Fig. 4 Local and Global Coordinates

The forces and displacements at a node, given in the global system, are transformed to the local system by employing a matrix [L] giving

$$\{\delta i\} = [L]\{\bar{\delta}_i\} \quad \text{and} \quad \{F_i\} = [L]\{\bar{F}_i\} \tag{57}$$

in which

$$[L] = \begin{pmatrix} \lambda & 0 \\ 0 & \lambda \end{pmatrix}, \tag{58}$$

where $[\lambda]$ is a three by three matrix of direction cosines of the angles formed between the two sets of axes. That is

$$[\lambda] = \begin{pmatrix} \lambda_{x\bar{x}} & \lambda_{x\bar{y}} & \lambda_{x\bar{z}} \\ \lambda_{y\bar{x}} & \lambda_{y\bar{y}} & \lambda_{y\bar{z}} \\ \lambda_{z\bar{x}} & \lambda_{z\bar{y}} & \lambda_{z\bar{z}} \end{pmatrix}. \tag{59}$$

In which $\lambda_{x\bar{x}}$ = cosine of the angle between the x and $\bar{x}$ axes, etc. These values can be determined from the coordinates of the nodes forming the element. For the whole set of forces

acting on the nodes of an element we can then write the equation in the form of equation (11), and finally obtain the stiffness matrix in global coordinates as equation (13)

$$[\bar{K}]^e = [T]^T [K]^e [T] \tag{13}$$

in which, matrix [T] is given by

$$[T] = \begin{bmatrix} L & 0 & 0 \\ 0 & L & 0 \\ 0 & 0 & L \end{bmatrix}. \tag{60}$$

e. Assembly of Elements

To obtain a complete solution for the entire structure, the two conditions of displacement compatibility and equilibrium have to be satisfied throughout. When any set of nodal displacements

$$\{\delta\} = \begin{Bmatrix} \delta_1 \\ \delta_2 \\ \cdot \\ \cdot \\ \delta_n \end{Bmatrix} \tag{61}$$

is listed for the whole structure in which all the elements participate, the condition of displacement compatibility is automatically satisfied. The overall equilibrium of the complete assemblage is provided by establishing equilibrium at the nodes of the structure. Consider the structure to be loaded by external forces [R]

$$\{R\} = \begin{Bmatrix} R_1 \\ R_2 \\ \cdot \\ \cdot \\ R_n \end{Bmatrix} \qquad (62)$$

applied at the nodes.

We now have to combine all the element properties into the stiffness matrix [K] for the complete structure. It is a matter of simply superimposing the element stiffness matrices in the appropriate positions of the matrix [K]. Then the force-displacement relation for the whole structure can be written as

$$\{R\} = [K]\{\delta\}. \qquad (63)$$

The solution for the unknown displacements can be obtained once the prescribed support displacements have been substituted into equation (63). The resulting displacements are referred to the global system, and before the stresses can be computed it is necessary to transform these into the local system for each element. The element stress matrix, equation (5), for 'in plane' bending components can then be used. In the existing program used in this report, the stresses are assigned to the centroid of each element and are converted to principal stresses and their directions.

4. Solution of Equations

The element stiffness matrices are formed one after the other, and then added to the appropriate locations of the overall matrix in accordance with the nodal numbers in the problem. Since the time necessary for inversion of a matrix increases approximately as the cube of the matrix size, a partitioning scheme is used to reduce the physical size of the stiffness matrix, equation (13). The final partitioned form of the overall stiffness matrix can be shown as in Fig. 5. Physically, this corresponds to the fact that the nodal points of the structure are divided into a number of partitions connected in series as illustrated in Fig. 6.

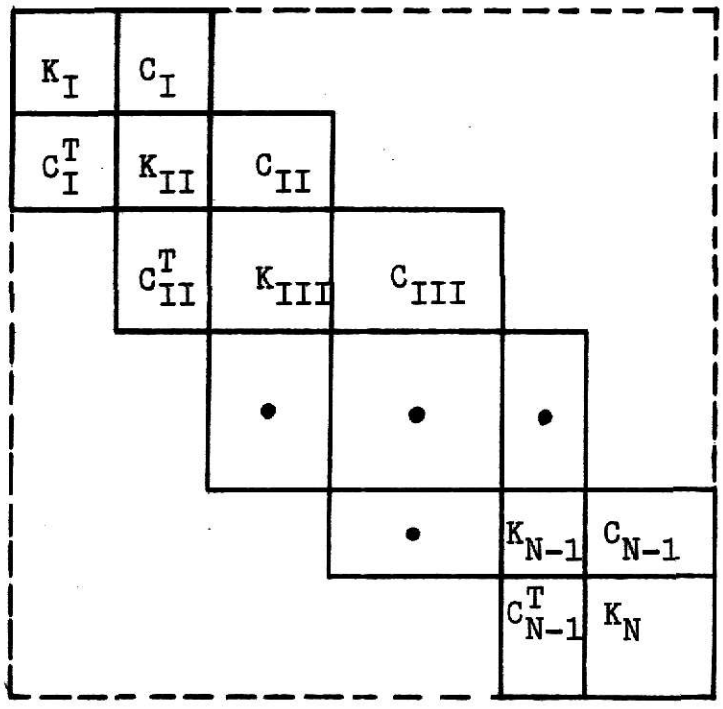

Fig. 5 Partitioned Stiffness Matrix

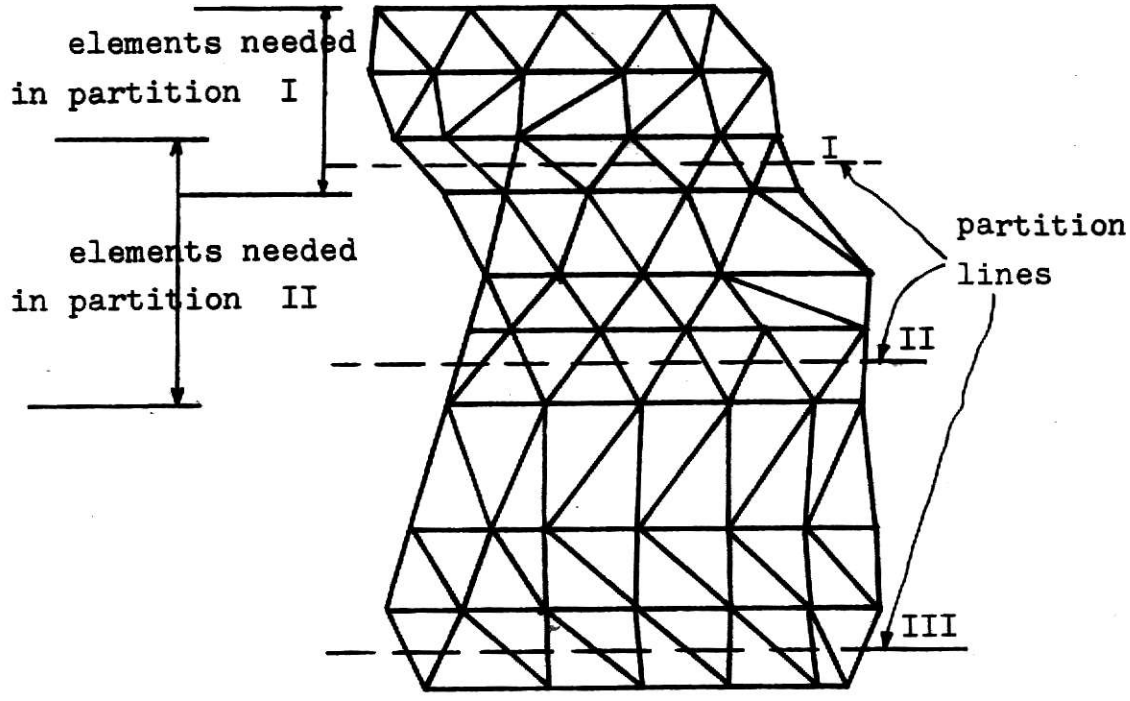

Fig. 6 Partitioning of A Structure

The final partitioned form of the overall matrix is sub-divided into convenient parts which are written in a tridiagonalized manner as follows:

$$\begin{bmatrix} K_I & C_I & 0 & 0 & \vdots & \vdots & 0 & 0 & 0 \\ C_I^T & K_{II} & C_{II} & 0 & \cdot & \cdot & 0 & 0 & 0 \\ 0 & C_{II}^T & K_{III} & C_{III} & \cdot & \cdot & 0 & 0 & 0 \\ \cdot & \cdot & \cdot & \cdot & \cdot & \cdot & \cdot & \cdot & \cdot \\ \cdot & \cdot & \cdot & \cdot & \cdot & \cdot & \cdot & \cdot & \cdot \\ 0 & 0 & 0 & 0 & \cdot & \cdot & K_{N-1} & C_{N-1} & \cdot \\ 0 & 0 & 0 & 0 & \cdot & \cdot & C_{N-1}^T & K_N & \cdot \end{bmatrix} \begin{Bmatrix} \delta_I \\ \delta_{II} \\ \delta_{III} \\ \cdot \\ \cdot \\ \delta_{N-1} \\ \delta_N \end{Bmatrix} = \begin{Bmatrix} P_I \\ P_{II} \\ P_{III} \\ \cdot \\ \cdot \\ P_{N-1} \\ P_N \end{Bmatrix} \quad (64)$$

This system of equations will be solved as follows:

The first two matrix equations can be written as

$$[K_I]\{\delta_I\} + [C_I]\{\delta_{II}\} = \{P_I\}$$
$$\text{and} \quad [C_I]^T\{\delta_I\} + [K_{II}]\{\delta_{II}\} + [C_{II}]\{\delta_{III}\} = \{P_{II}\}. \tag{65}$$

The first equation will yield

$$\{\delta_I\} = [K_I]^{-1}\{P_I\} - [K_I]^{-1}[C_I]\{\delta_{II}\} \tag{66}$$

and substituting into the second yields

$$([K_{II}] - [C_I]^T[K_I]^{-1}[C_I])\{\delta_{II}\} + [C_{II}]\{\delta_{III}\}$$
$$= \{P_{II}\} - [C_I]^T[K_I]^{-1}\{P_I\}. \tag{67}$$

By defining new symbols,

$$[\bar{K}_{II}] = ([K_{II}] - [C_I]^T[K_I]^{-1}[C_I]) \text{ and}$$
$$\{\bar{P}_{II}\} = \{P_{II}\} - [C_I]^T[K_I]^{-1}\{P_I\} \tag{68}$$

equation (67) may be written as

$$[\bar{K}_{II}]\{\delta_{II}\} + [C_{II}]\{\delta_{III}\} = \{\bar{P}_{II}\}, \tag{69}$$

from which $\{\delta_{II}\}$ can be obtained as $\{\delta_I\}$ is found in equation (66) and then substituted into the next row equation to give $[\bar{K}_{III}]$ and $\{\bar{P}_{III}\}$.

This process of substitution and elimination goes on until the last row is reached, that is,

$$[\bar{K}_N]\{\delta_N\} = \{\bar{P}_N\} \tag{70}$$

where a direct inversion will yield $\{\delta_N\}$.

The process is then reversed and the known displacement values are back-substituted into equations in the form of equation (66), giving solutions for all of the unknowns.

To check the errors introduced in the solution of equation (64), the residuals are calculated as

$$\{R\} = \{P\} - [K]\{\delta\} . \tag{71}$$

NUMERICAL EXAMPLES

1. Experimental Setup

As described in Reference (1) two simply supported W shape 12x45 steel beams were each subjected to a concentrated load at midspan. The centerline of the web opening was 20 inches from the midspan. Each beam was tested with four values of moment-shear ratio at the opening by varying the length of the shear span from 100 inches to 40 inches in increments of 20 inches as shown in Fig. 7.

The web opening which was located on the centroidal axis of the beam was 6 in deep and 9 in long with a 1/2 inch corner radius as indicated in Fig. 8(a). Thus, the width-to-depth ratio of the opening was 1.5 and the nominal ratio of depth of opening to depth of beam was 0.5.

One beam was tested without reinforcing and several were tested with horizontal reinforcing strips placed around the opening. The reinforcing details for the beam of interest are shown in Fig. 8(a) and (b). The cross sectional dimensions of the beam used in this study were the nominal values as indicated in Fig. 8(c). The modulus of elasticity was 29,000 ksi and the Poisson's ratio was taken as 0.3.

2. Solution By Superposition

In order to investigate the stress distribution around the web opening by the finite element method a portion, A-B, was assumed cut out of the beam as shown in Fig. 9(a). The 36 inch section, A-B, was assumed to extend far enough past the hole on either side that the actual stress condition in the section as it

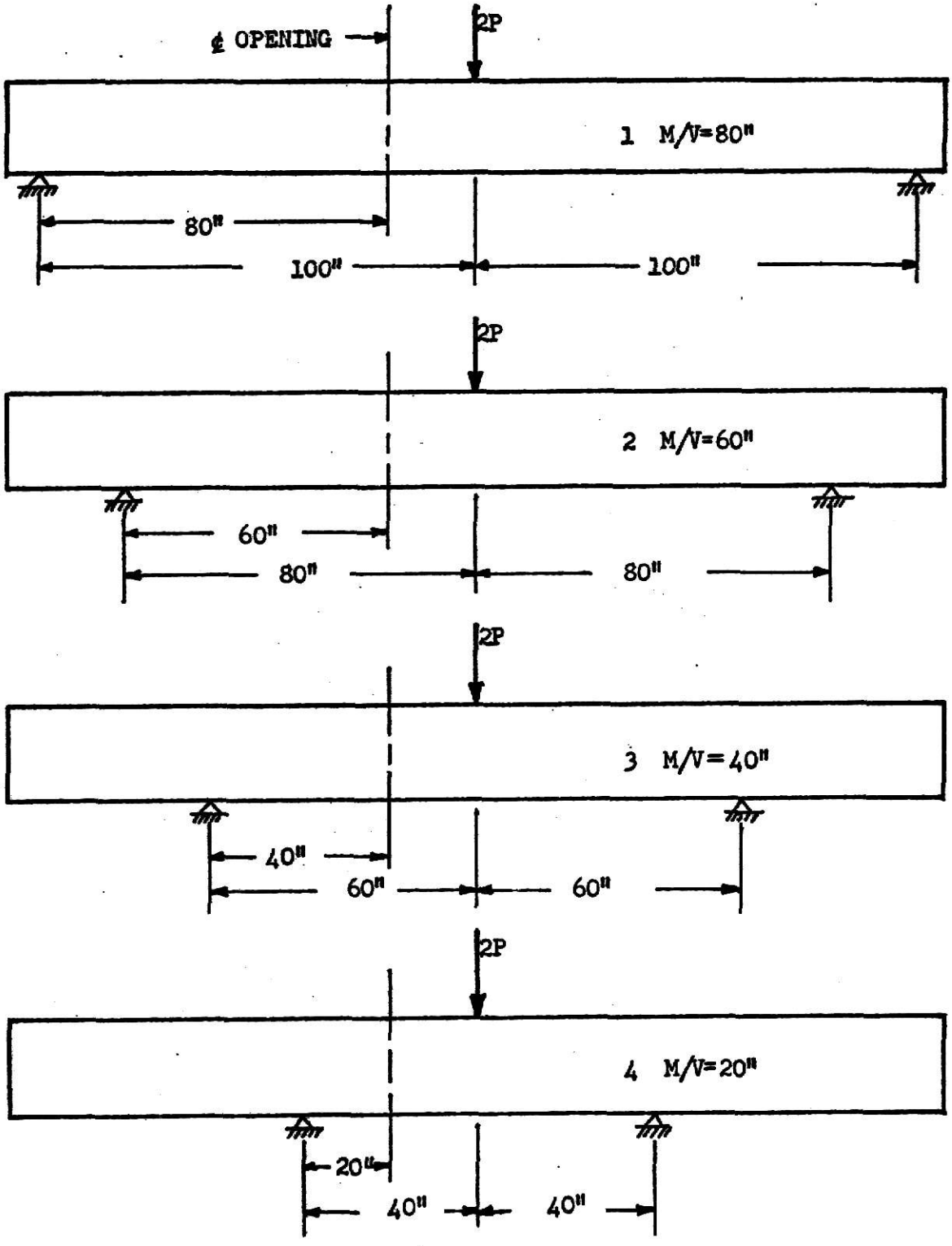

Fig. 7 Experimental Setups

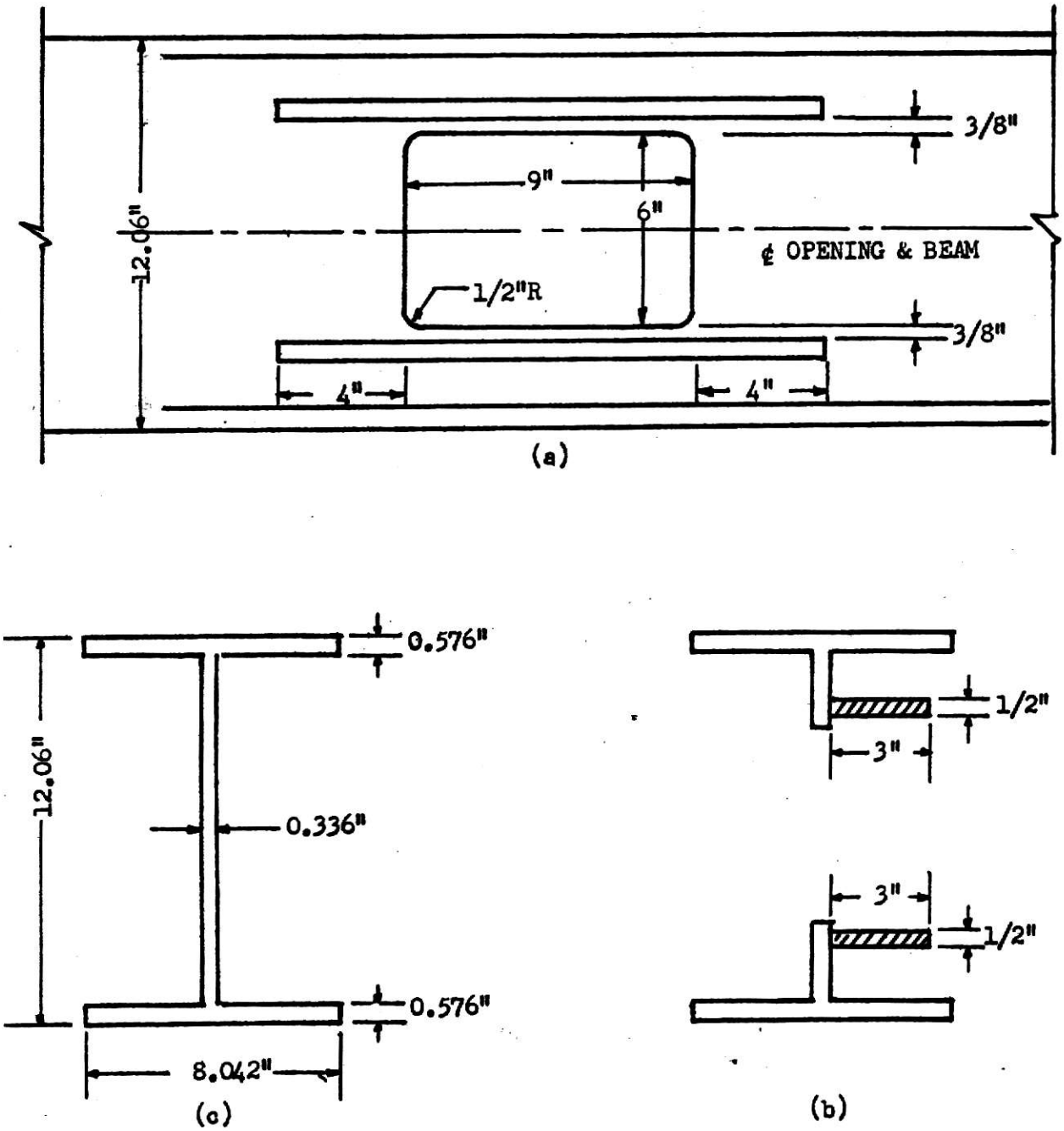

Fig. 8 Web Opening And Reinforcing Details

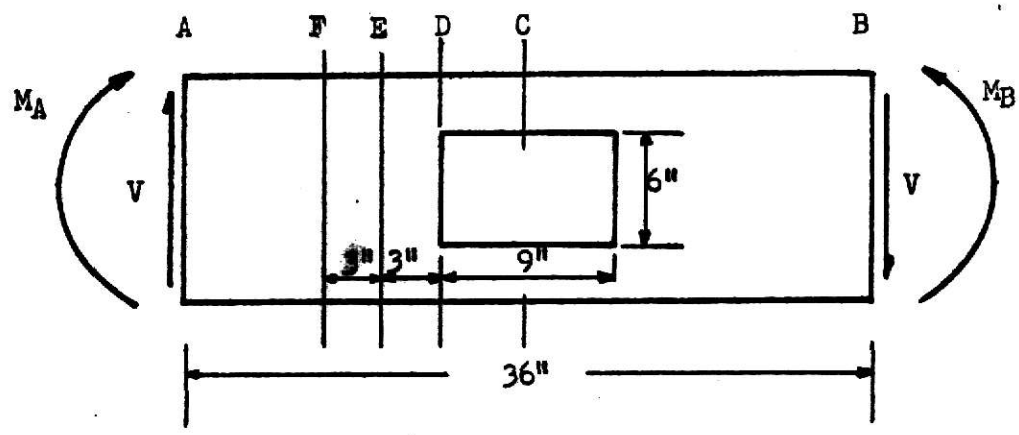

(a) Analyzed Section

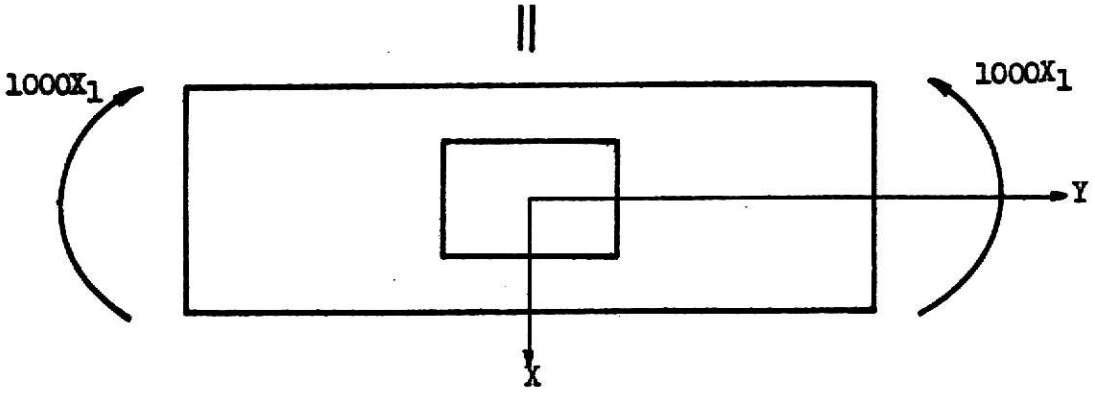

(b) Pure Bending

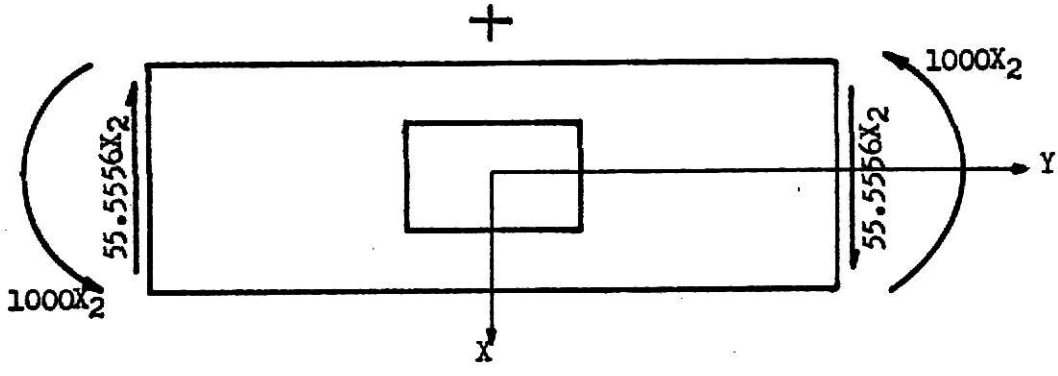

(c) Bending With Shear

Fig. 9 Statically Equivalent Loads For Analyzed Section

existed in the beam would be approximated by applying the nominal end moments and shears to the section as a free body.

For the analysis of each beam (with and without reinforcing), a superposition technique was used in order to save computer time. The section A-B subjected to end shears and moments is statically equivalent to the same section subjected to pure bending plus shear with bending as indicated in Fig. 9. By static theory, the factors X_1, X_2 can be evaluated for any moment-shear ratio by solving the following two simultaneous equations

$$1000\ X_1 - 1000\ X_2 = M_A$$

$$1000\ X_1 + 1000\ X_2 = M_B$$

For both cases, there were four values of the moment-shear ratio. The resulting factors are listed in Table 1 and Table 2 respectively.

For each beam, thus, we need only analyze the two sections loaded by end moments of 1000 k-in in the first case and by end moments of 1000 k-in and end shears of 55.55 kips for the second case, arranged as in Fig. 9(b) and (c). These results multiplied by the appropriate factors X_1, X_2 and superimposed, yield the complete solution for the various values of the moment-shear ratio.

2P=12 kips					
M/V (in)	V (k)	M_A (k-in)	M_B (k-in)	X_1	X_2
80	6	372	588	0.48	0.108
60	6	252	468	0.36	0.108
40	6	132	348	0.24	0.108
20	6	12	228	0.12	0.108

Table 1. Factors for Beam without Reinforcing

2P=24 kips					
M/V (in)	V (k)	M_A (k-in)	M_B (k-in)	X_1	X_2
80	12	744	1176	0.96	0.216
60	12	504	936	0.72	0.216
40	12	264	696	0.48	0.216
20	12	24	456	0.24	0.216

Table 2. Factors for Beam with Reinforcing

3. Finite Element Solution

a. Displacement Boundary Conditions

For the pure bending case, Fig. 9(b), the behavior is symmetrical with respect to the X axis and antisymmetrical with respect to the Y axis. For the bending with shear case, Fig. 9(c) the behavior is antisymmetrical with respect to both the X and Y axes. Under these conditions, it was possible to analyze only

one-quarter of the section by introducing appropriate restraint conditions on the boundary nodes as illustrated in Figs.10 and 11.

b. Element Discretization

For the case without reinforcing the area of interest was divided into a finite element mesh of 50 triangular elements and 35 nodal points. This mesh is shown in Fig. 12. Smaller triangular elements were used near the perimeter of the hole in order to get a better picture of stress distribution near the hole. The rounded corners could not be approximated in this analysis since the mesh size was too large. However, the fillets would affect the stress distribution very little except in the immediate vicinity of the opening. The nodal points were assigned consecutively to 2 partitions. The partitions are indicated in Fig. 12 by Roman numerals and dashed lines.

For the case with reinforcing strips, the area of interest was also divided a mesh. This mesh contained 58 triangular elements and 40 nodes and is shown in Fig. 13. The triangular elements on the web and flange were the same as those of the previous case. The nodal points were assigned consecutively to 3 partitions. The partitions are indicated in Fig. 13 by Roman numerals and dashed lines. The heavy lines indicate the common boundary lines of the flange and the web and the reinforcing and the web. The exact length of the reinforcing used in the experimental analysis did not fit the nodal point exactly. In this analysis the reinforcing used was 1/2 " longer than the actual length. The space between the reinforcing and the edge

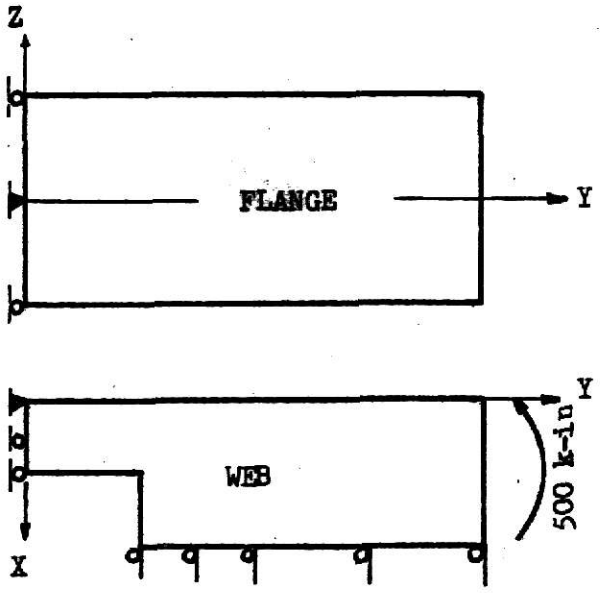

Release along the Z axis in the X and Z directions except for the origin.

Release along the X axis and along the longitudinal center line in the X direction except for the origin.

a. Pure Bending

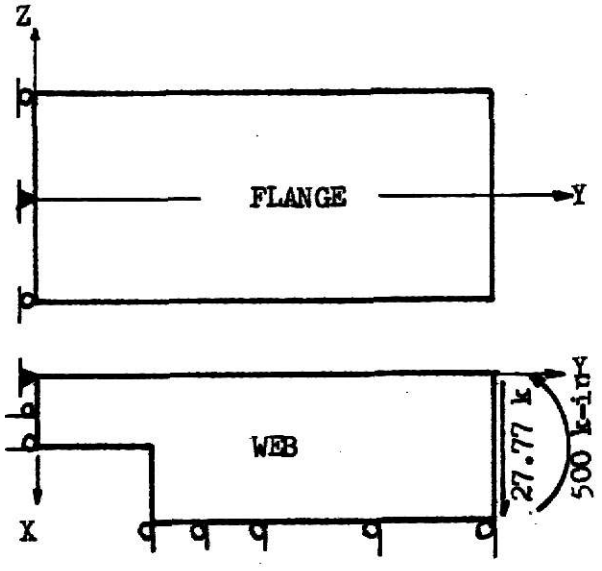

Release along the Z axis in the Z and M_z directions except for the origin.

Release along the X axis in the Y direction.

Release along the longitudinal center line, in the X direction.

b. Bending With Shear

Fig. 10 Boundary Conditions For Beam Without Reinforcing

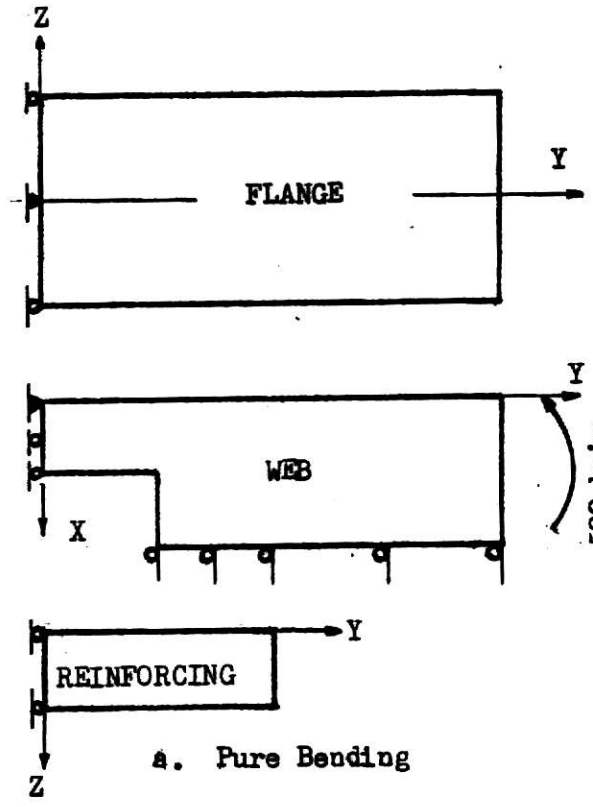

a. Pure Bending

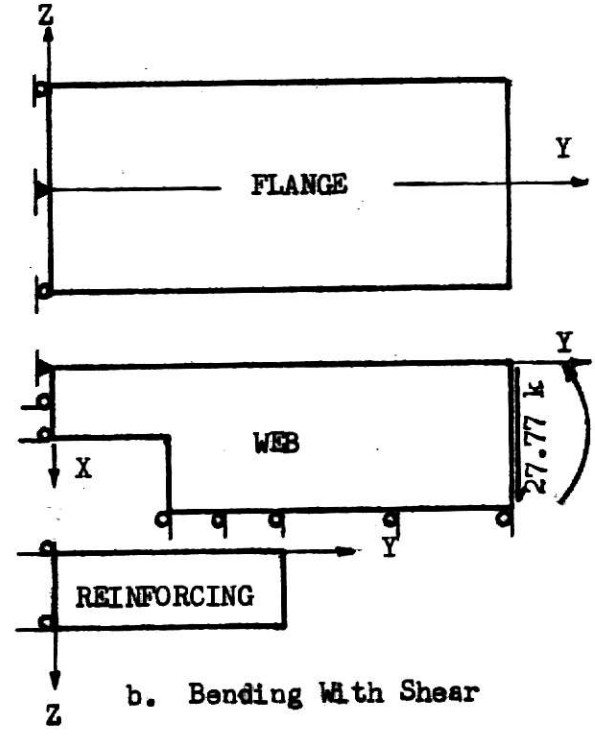

b. Bending With Shear

Fig. 11 Boundary Conditions For Beam With Reinforcing

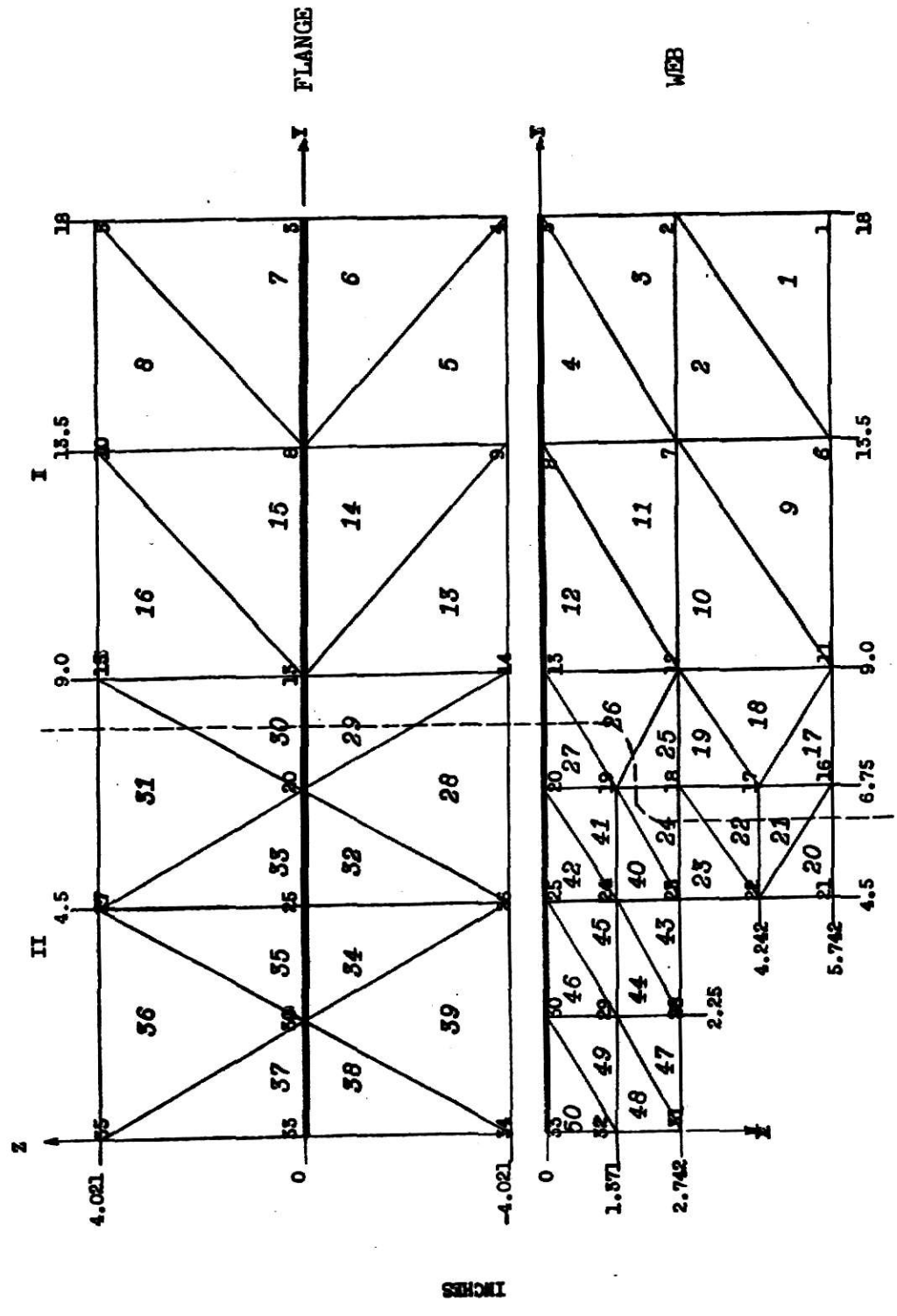

Fig. 12 Element Discretization For Beam Without Reinforcing

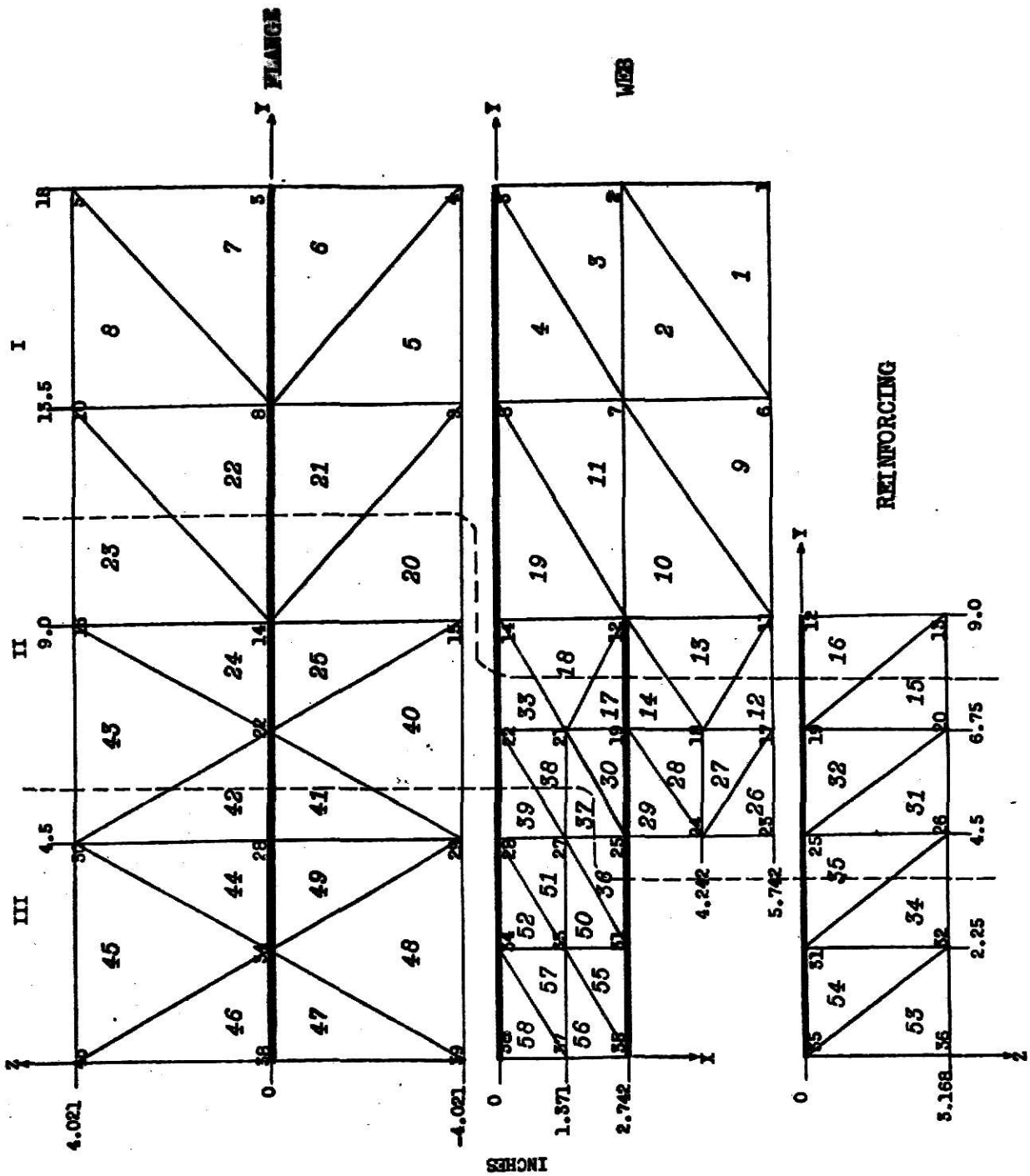

Fig. 13 Element Discretization For Beam With Reinforcing Strips

of the opening was omitted since the element size was such that this was the most reasonable location for the reinforcing.

C. Consistent Nodal Loads

The moments and shear forces on the free body, Fig. 10 and Fig. 11, could not be used directly. These moment and shear were approximated by a series of concentrated loads applied at the nodal points on the end section in this analysis. The flexural stress at the end section was calculated by the simple beam theory,

$$\sigma = \frac{M\,C}{I}$$

Since the stress varies linearly along the boundary, the consistent nodal forces were the static resultants of this stress distribution. The general expressions for the concentration formula for a linearly varying distribution are listed below.

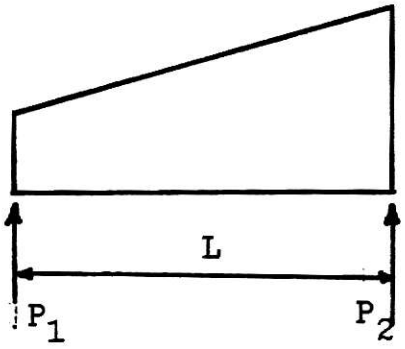

$$P_1 = \frac{L\,t}{6}(2p_1 + p_2)$$

$$P_2 = \frac{L\,t}{6}(2p_2 + p_1)$$

p_i = force intensity per unit area

t = thickness

The concentrated load at each nodal point was the sum of the static resultants from the adjacent sides. The small difference between the sum of the moments produced by these concentrated

forces, applied at the nodal points, about the neutral axis and the statical moment at the section was proportionately resolved into a series of small concentrated loads, which were then added to the previous concentrated loads making the sum of the moments produced by these nodal forces equal to the statical moment, 500 k-in. These concentrated loads are shown in Fig. 14(a).

The shear stress was calculated by the usual equation

$$v = \frac{V\,Q}{b\,I}$$

and the static resultants for the parabolic variation are shown below.

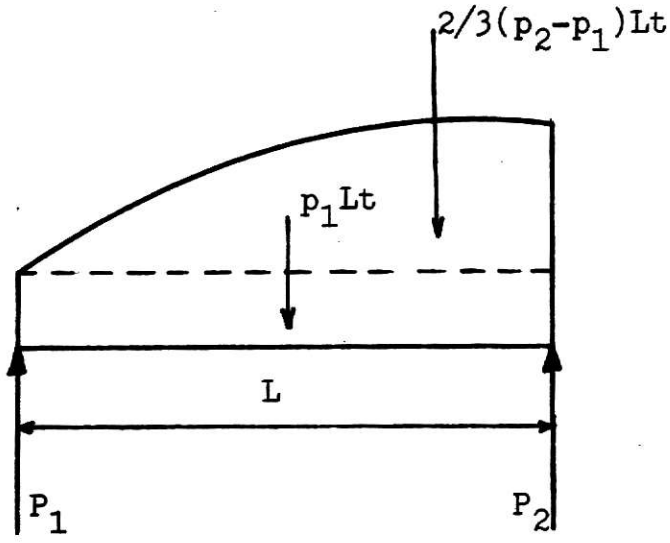

$$P_1 = \frac{p_1 L\,t}{2} + \frac{1}{4} L^2 t\,(p_2 - p_1)$$

$$P_2 = \frac{p_1 L\,t}{2} + \frac{5}{12} L^2 t\,(p_2 - p_1)$$

p_i = shear stress per unit area

t = thickness

The equivalent nodal forces at each node are the sum of the static resultants from the adjacent sides. The shear stress on the flange was assumed to be concentrated at the center point of the flange. The equivalent nodal loads are shown in Fig. 14 (b).

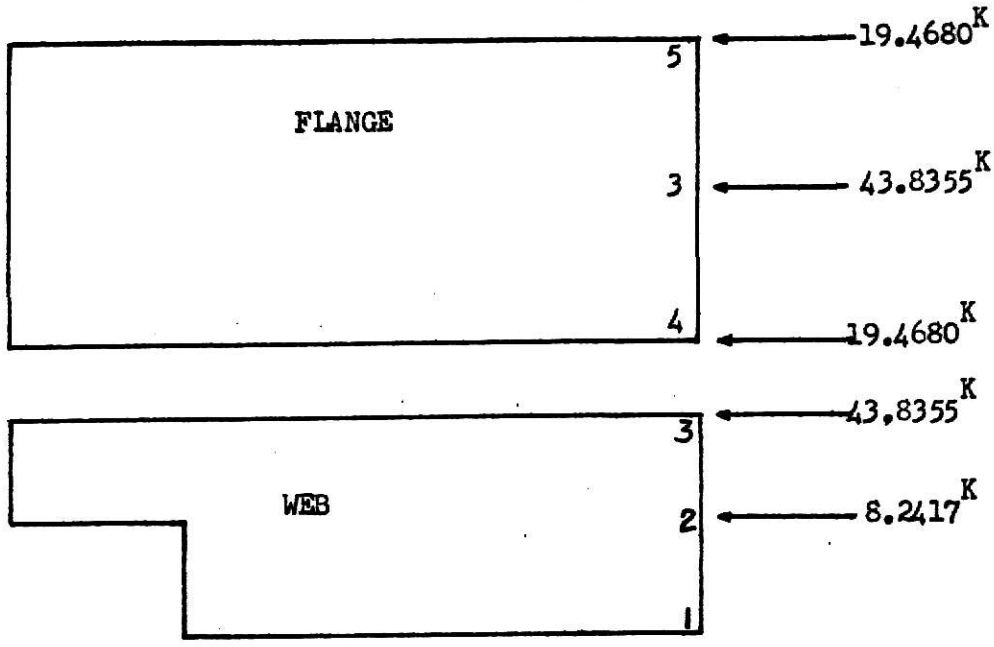

(a) Equivalent Nodal Forces For Bending Moment

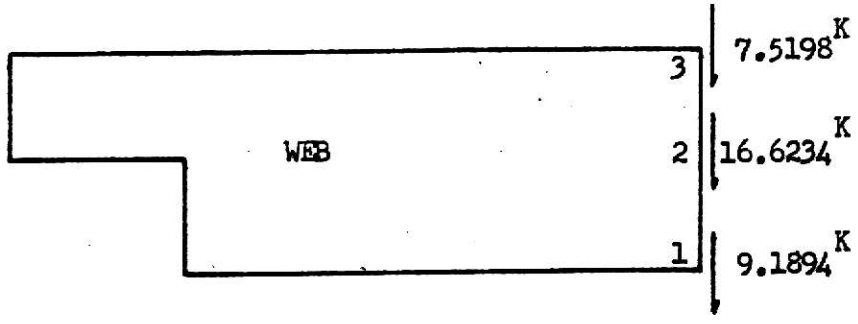

(b) Equivalent Nodal Forces For Shear Forces

Fig. 14 Equivalent Nodal Forces Used In Finite Element Method

PRESENTATION AND DISCUSSION OF RESULTS

1. Normal Stresses

Figures 15 through 30 present a comparison of the normal stresses due to in plane bending obtained from the finite element method based on the mesh of Figs. 12 and 13, with the experimental values (1) and the theoretical analysis based on the 'Vierendeel Method' (1).

The dots and solid lines in the figures represent the results using the finite element analysis. Since the method of finite elements used is an averaging procedure, the stresses obtained with constant strain triangles do not reflect the actual stress for any particular point, but are constant throughout an element. It is usual to assign the calculated stress values to the element centroids and then to interpolate linearly to estimate the stress for a particular point. Using this procedure, the normal stresses were plotted on the figures for sections C, D and E (Fig. 9a), and the solid lines passing by those dots approximate the calculated stress variation for the given sections. The points indicated by the small crosses represent the experimental values and the dashed lines in the figures represent the Vierendeel analysis values as given in Reference (1).

From these figures, it can be seen that the normal stresses obtained using the finite element analysis agree quite well with the experimental data along section C (the centerline of the

opening) for both the reinforced and the unreinforced cases, and are also in good agreement with the predictions based on the Vierendeel Analysis.

Along section D (the edge of the opening), the stresses calculated from the finite element approach, agree reasonably well with the experimental data except at the edges of the opening and at the flange. Because of the relatively large element size used in this report, it is difficult to get a good approximation of the stress variation near the opening. The dashed lines have been extended from the solid lines in order to approximate the stresses near the edge. To get more reasonable approximate values around this region, the area of interest should be further subdivided. As for the top flange, the stress plotted is the average value of the adjacent elements at the middepth of the flange, that represent the average value at the flange. There is no way to get the value at the top edge of the flange. As can be seen from those figures, the finite element approach results in a more reasonable and accurate normal stress distribution than the Vierendeel Analysis along section D.

The normal stresses calculated by the finite element method along section E (3" from the opening), as shown in Figs. 16, 18, 20, 22, 24, 26, 28 and 30 were also in all cases close to the experimental data. The Vierendeel Analysis was not applied to this region.

2. Bending Stresses

For the beams with one-sided reinforcing strips, bending stresses are induced in the web due to the unsymmetrical transverse sections stiffened by the longitudinal reinforcing strips. The bending stresses in the web are shown in Figs. 31, 32, 33 and 34. As shown in these figures, the maximum average bending stress occurs at the corner of the opening, where the stress concentration occurs. The comparison of this maximum average bending stress with the maximum normal stress in the vicinity of the corner showes the bending stress to be approximately 5.5 percent of the maximum normal stress. From this comparison, it may be concluded that the use of one-sided reinforcing strips had no significant effect on the normal stresses in the web.

3. Shear Stresses

In order to compare the results of this study with the data given in Reference (1), the shear stresses obtained from the individual results of a series were averaged to represent the results for the series. Then the average values of the adjacent elements were used to represent the stress distribution for the sections of interest as shown in Fig. 35 by dots and solid lines. The dashed lines in the figure represent the theoretical values based on simple beam theory, $S_{xy} = \frac{V\,Q}{I\,b}$ (1). The points indicated by small crosses represent the experimental data (1). It can be seen from Fig. 35 that, for the unreinforced opening, the results of the finite element analysis are in good agreement

with the experimental data, except at section C. At section C the stress distribution pattern is similar to the distribution predicted by $v = \frac{V Q}{I b}$. However the magnitude of the calculated stress is significantly higher than the experimental value. It should be noted that the experimental data collected at this point on the unreinforced beam tended to be low for all cases.

For the opening, with one-sided reinforcing as shown in Fig. 35, reasonable agreement was obtained for all sections between the finite element analysis and the experimental data. From the comparison of the results, it can be concluded that the finite element method can predict reasonably accurate stress distributions for this class of problems.

CONCLUSIONS

From the comparison of the results obtained by the finite element method with the experimental and theoretical values, some conclusions can be reached:

1. The normal stresses obtained using the finite element analysis were in good agreement with the experimental data for the unreinforced cases and for the one-sided reinforced cases under the four given moment-shear ratios.

2. Along the section at the centerline of the opening, the normal stresses obtained using the finite element analysis were close to the predictions based on the so-called 'Vierendeel Analysis'. Away from that section, the finite element approach predicts more reasonable and accurate stress distributions than those predicted by the Vierendeel Analysis for all cases.

3. The use of one-sided reinforcing strips had little effect on the stress distribution since the bending stresses induced in the web were relatively small when compared with the normal stresses.

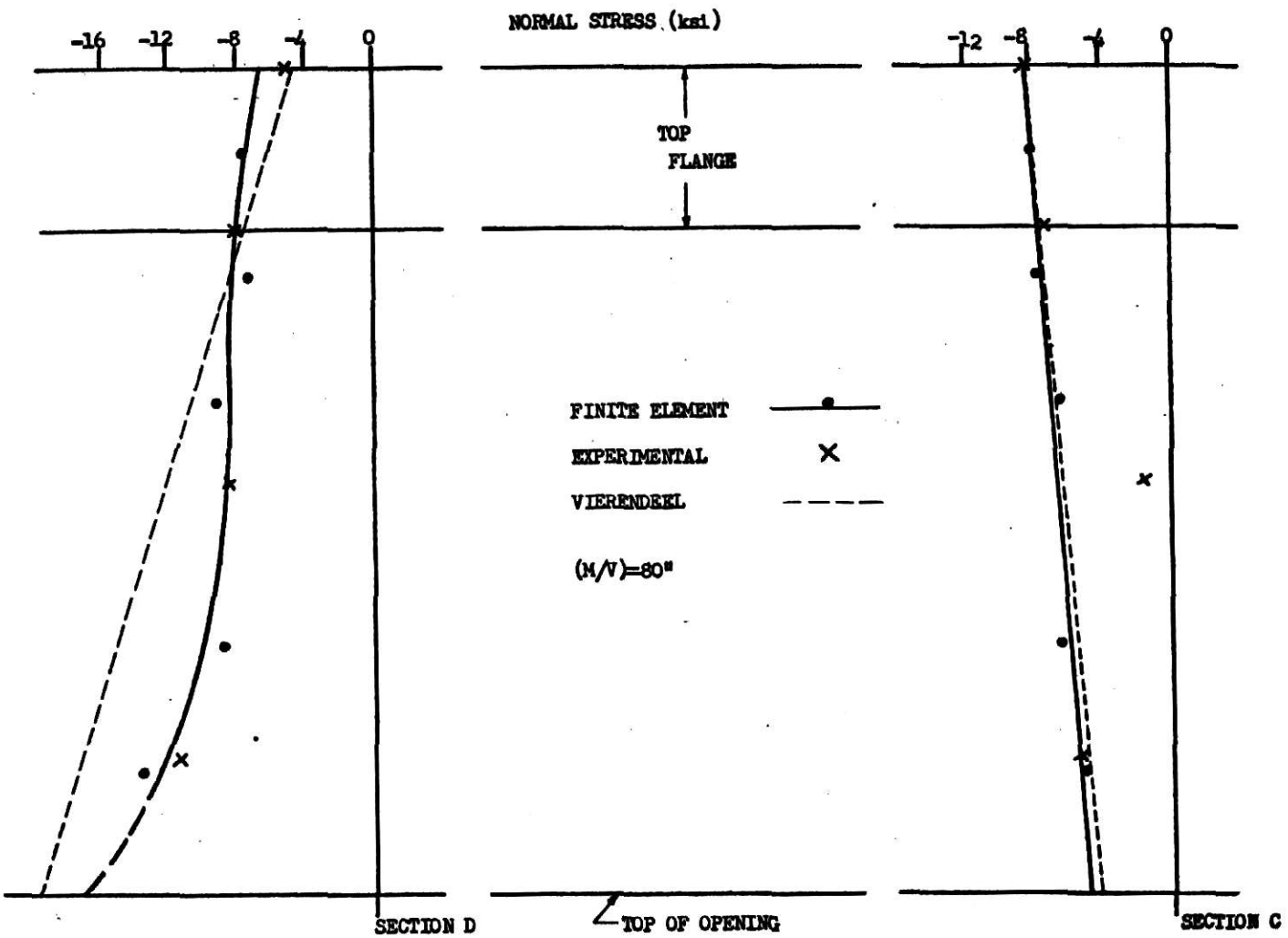

Fig. 15 Normal Stresses For Beam Without Reinforcing

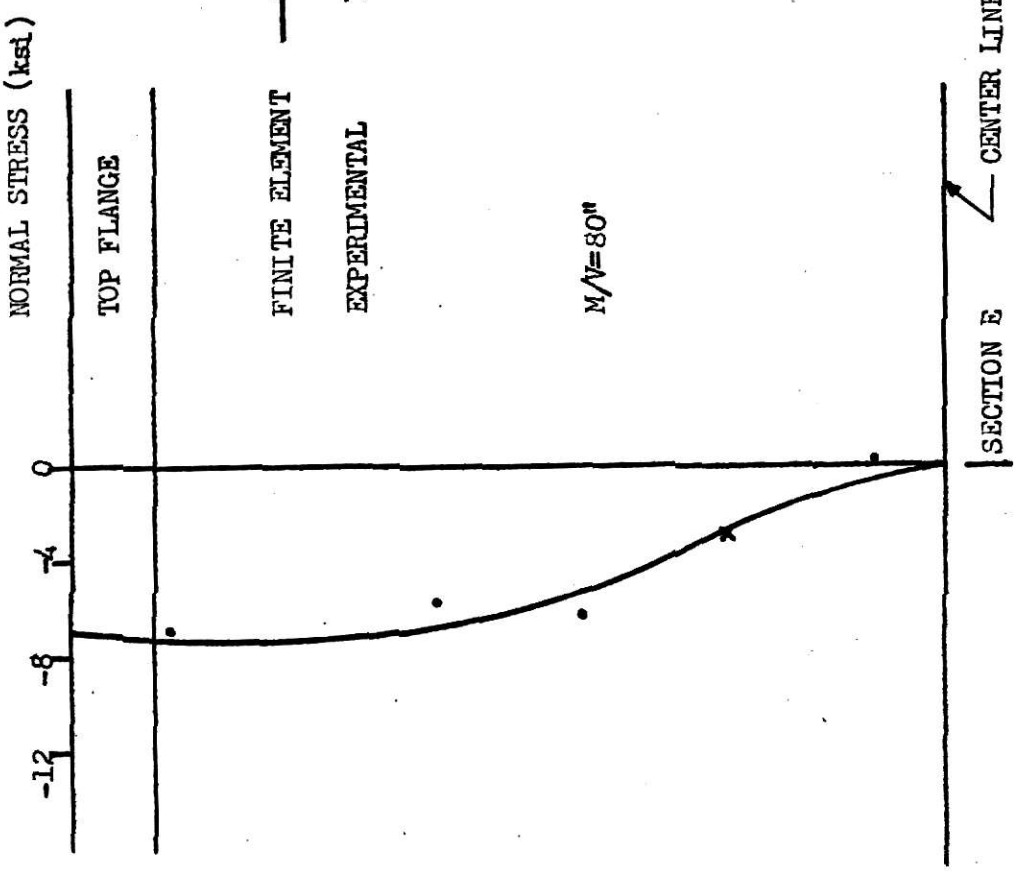

Fig. 16 Normal Stresses For Beam Without Reinforcing

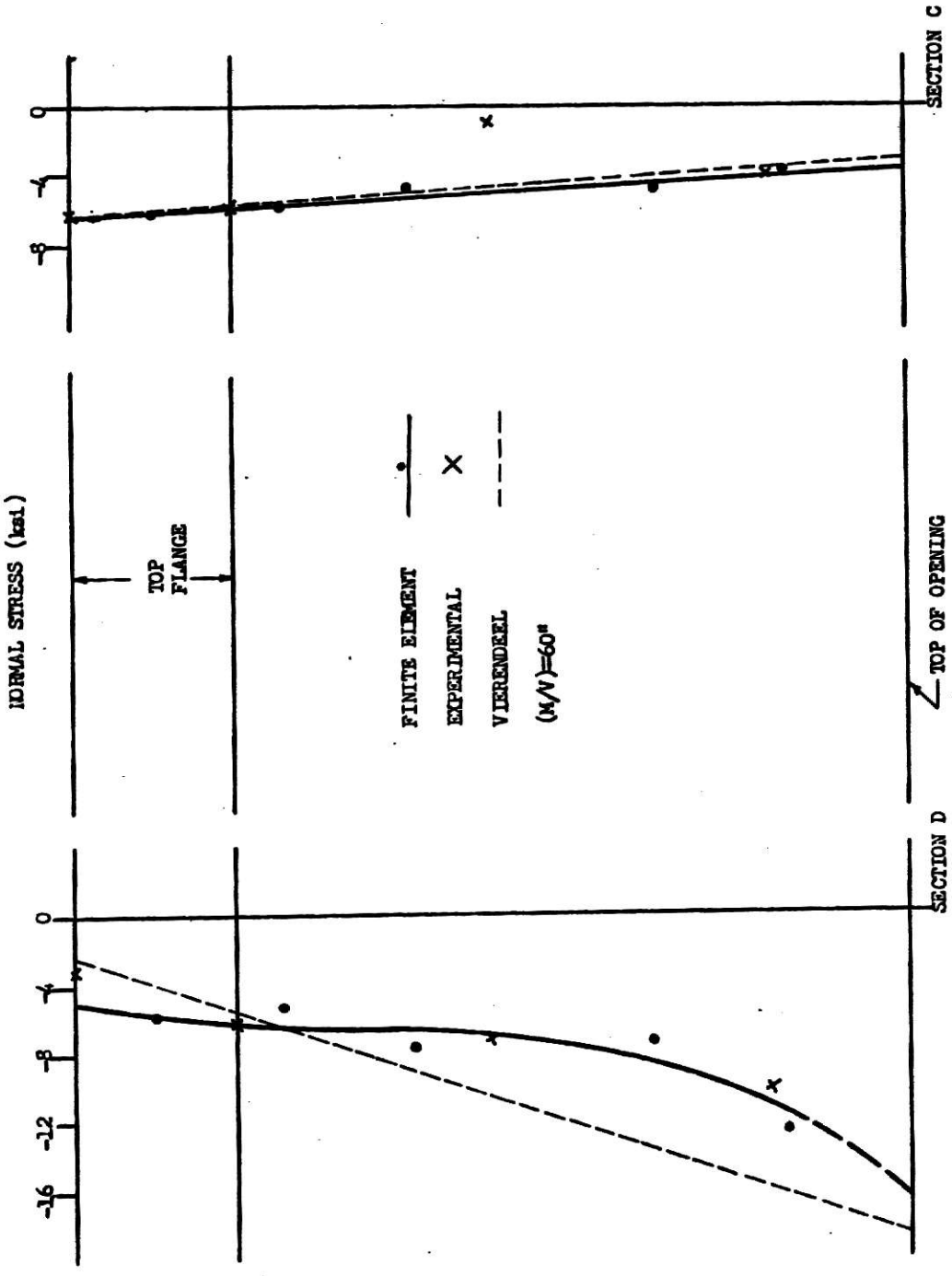

Fig. 17 Normal Stresses For Beam Without Reinforcing

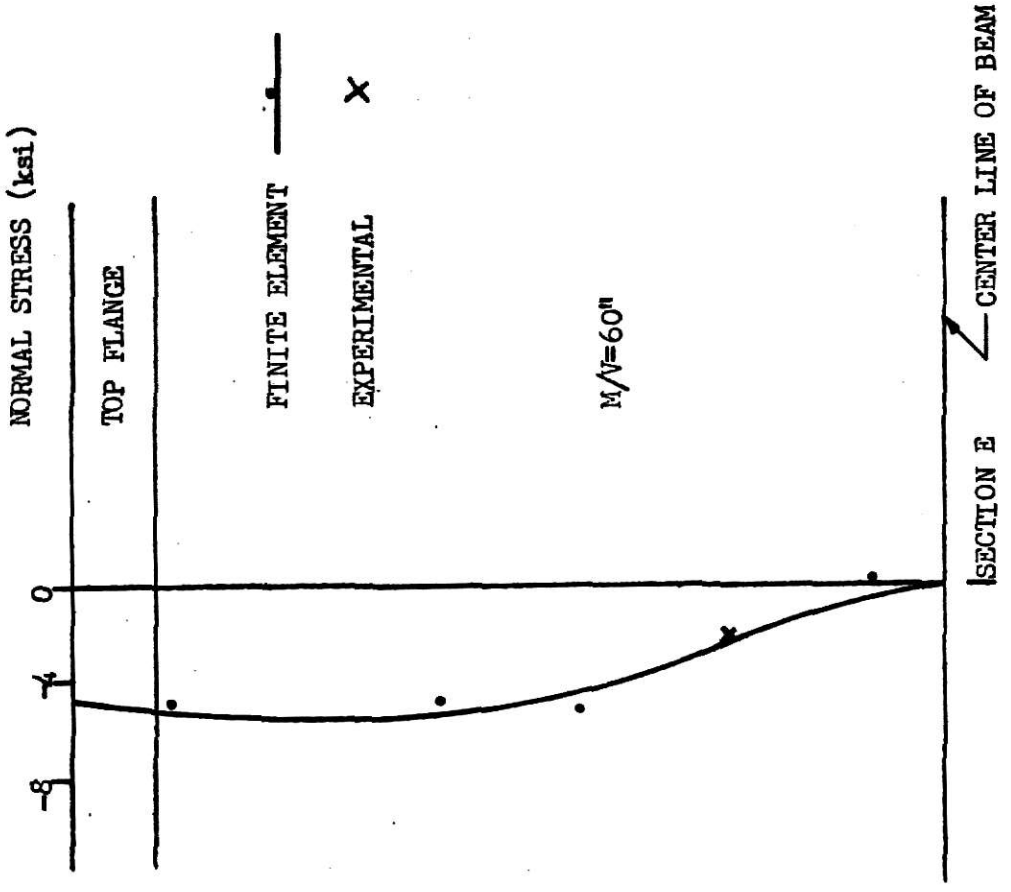

Fig. 18 Normal Stresses For Beam Without Reinforcing

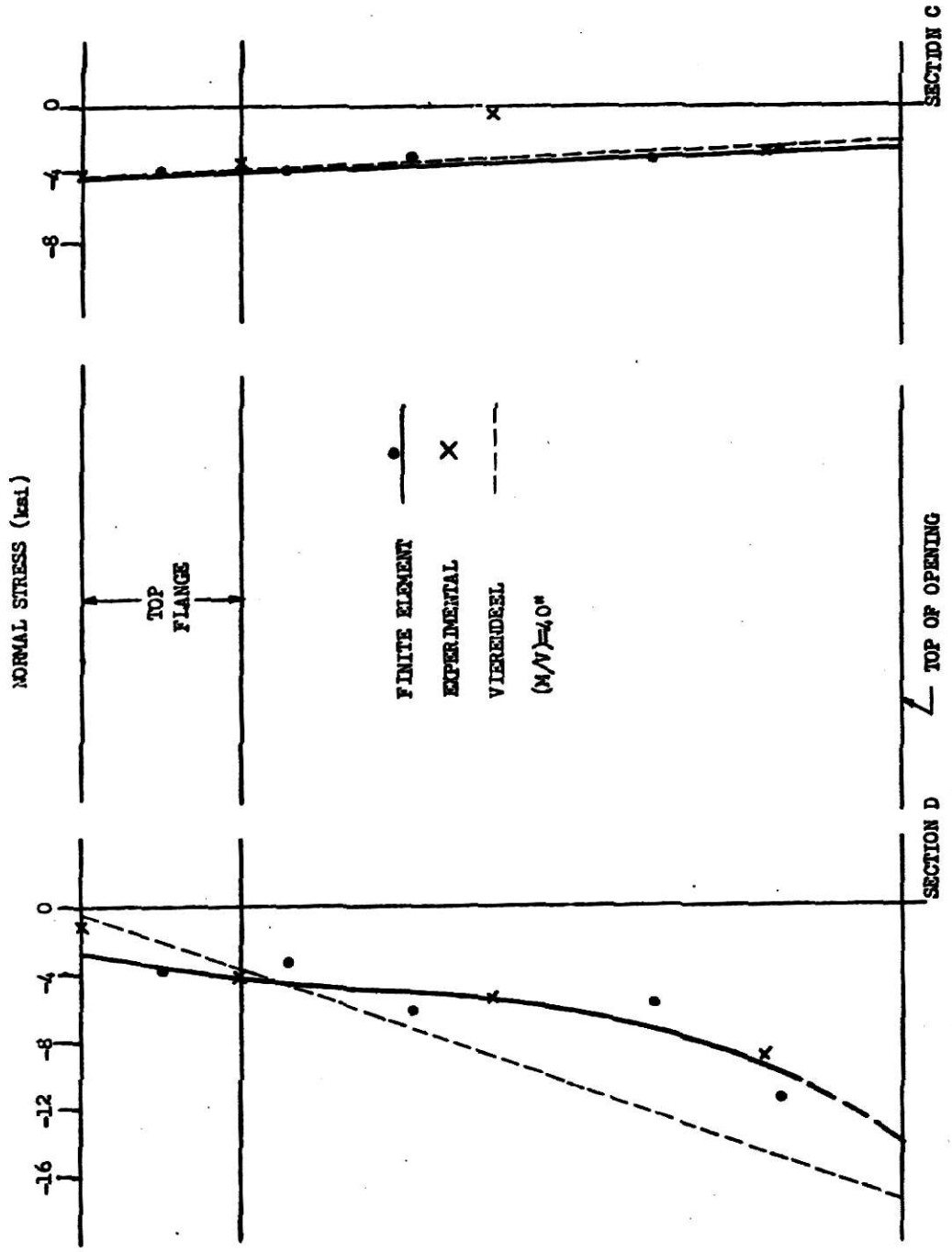

Fig. 19 Normal Stresses For Beam Without Reinforcing

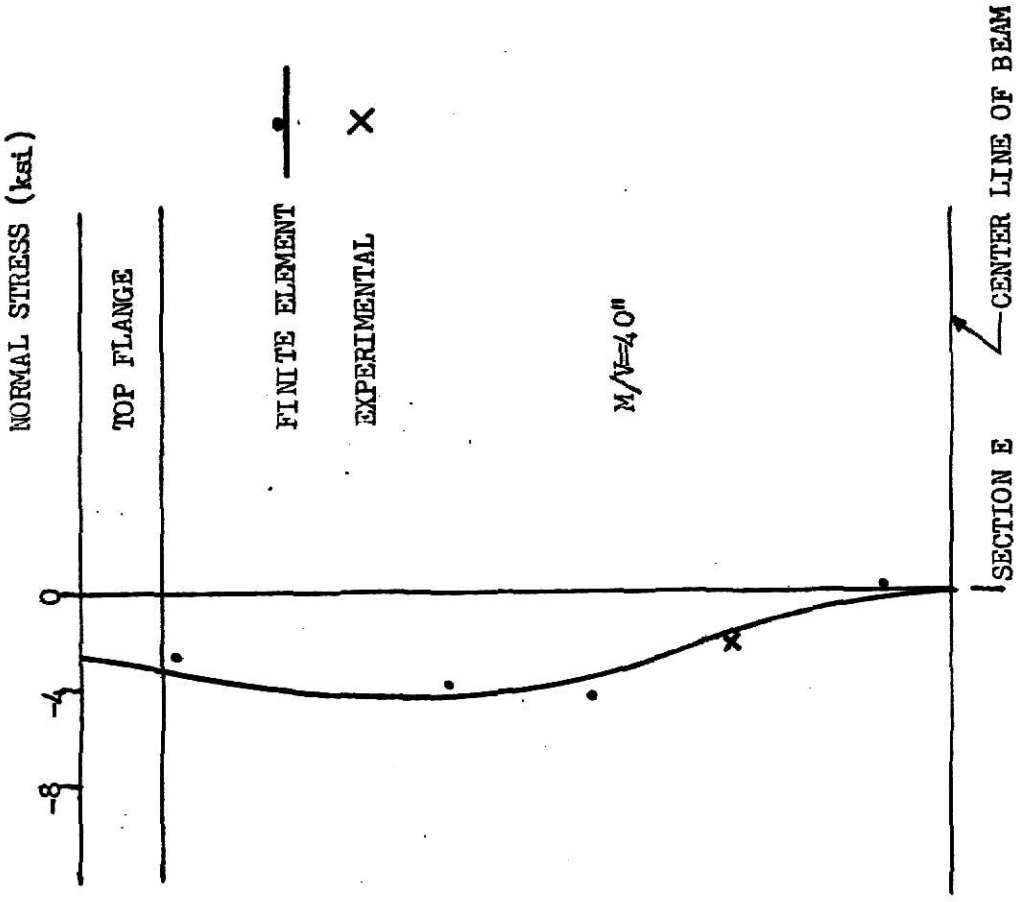

Fig. 20 Normal Stresses For Beam Without Reinforcing

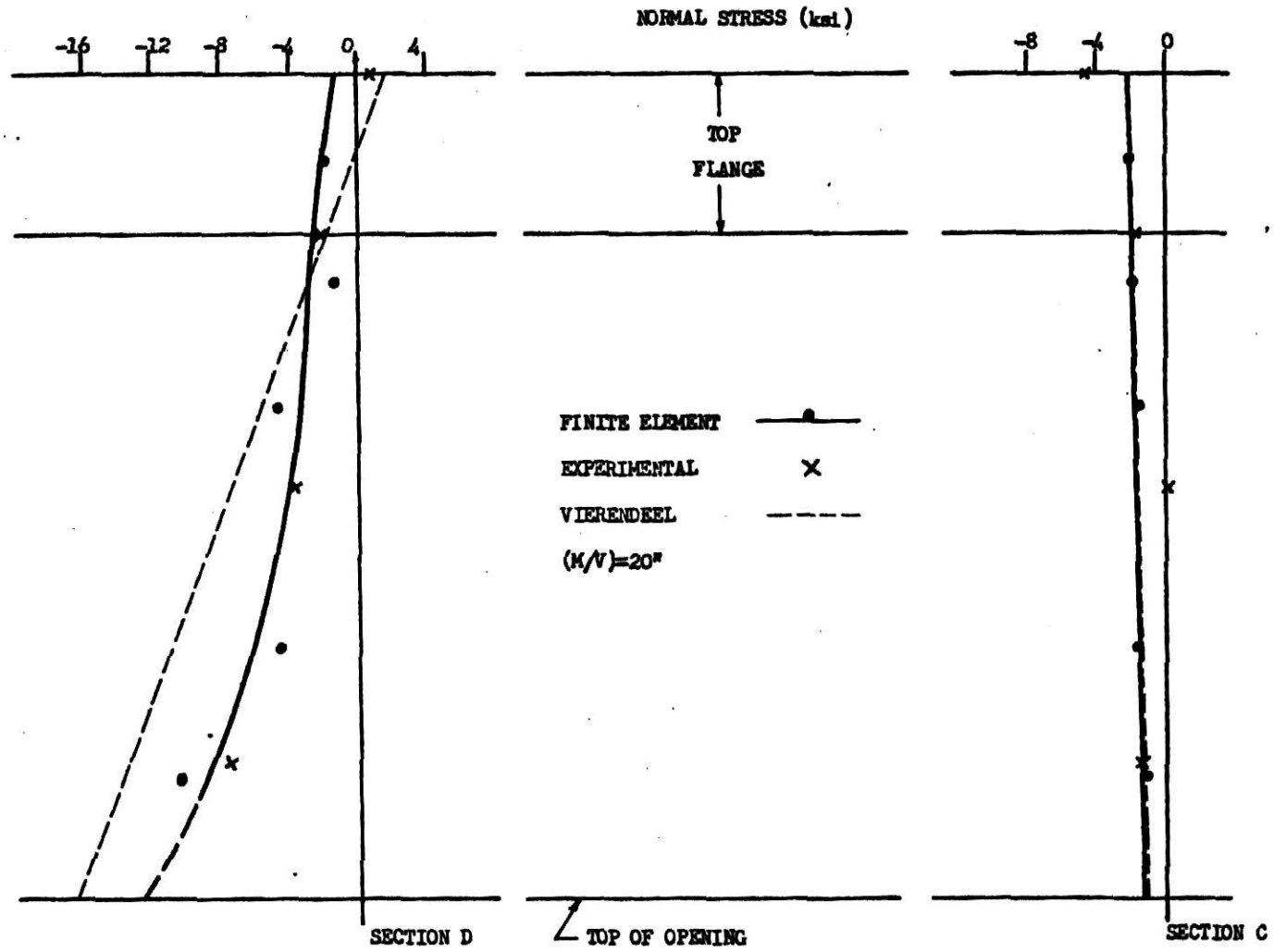

Fif. 21 Normal Stresses For Beam Without Reinforcing

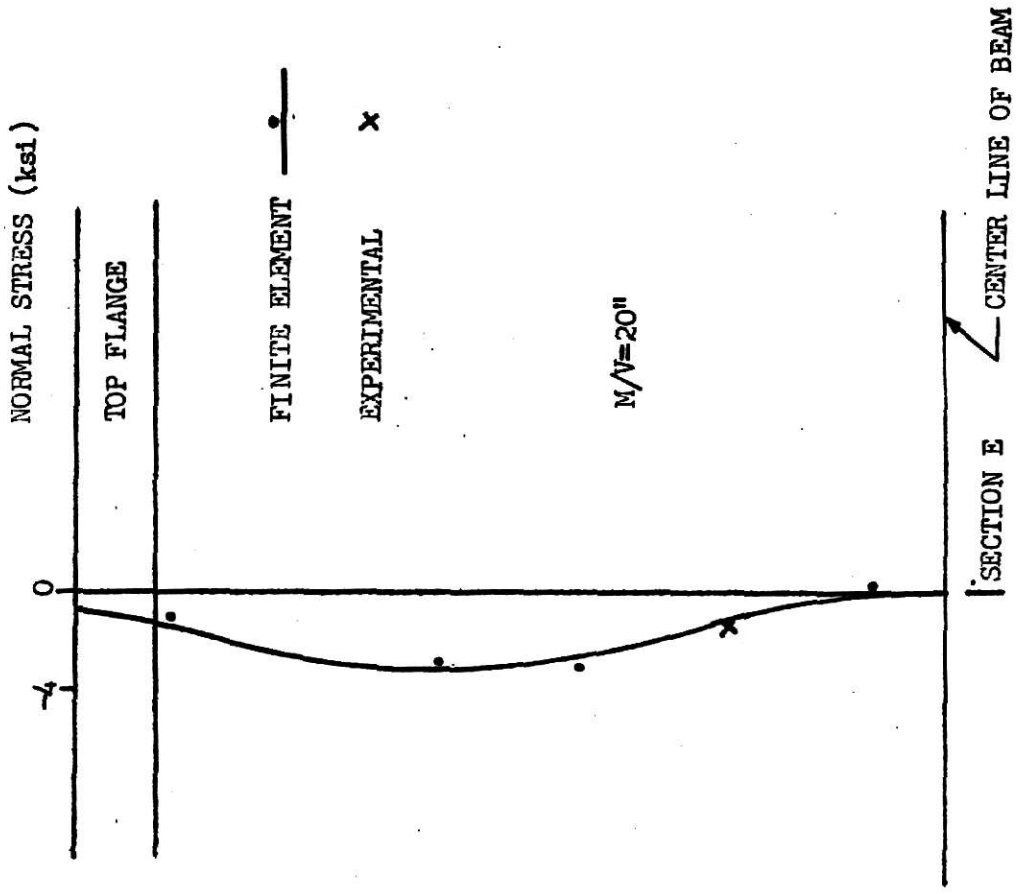

Fig. 22 Normal Stresses For Beam Without Reinforcing

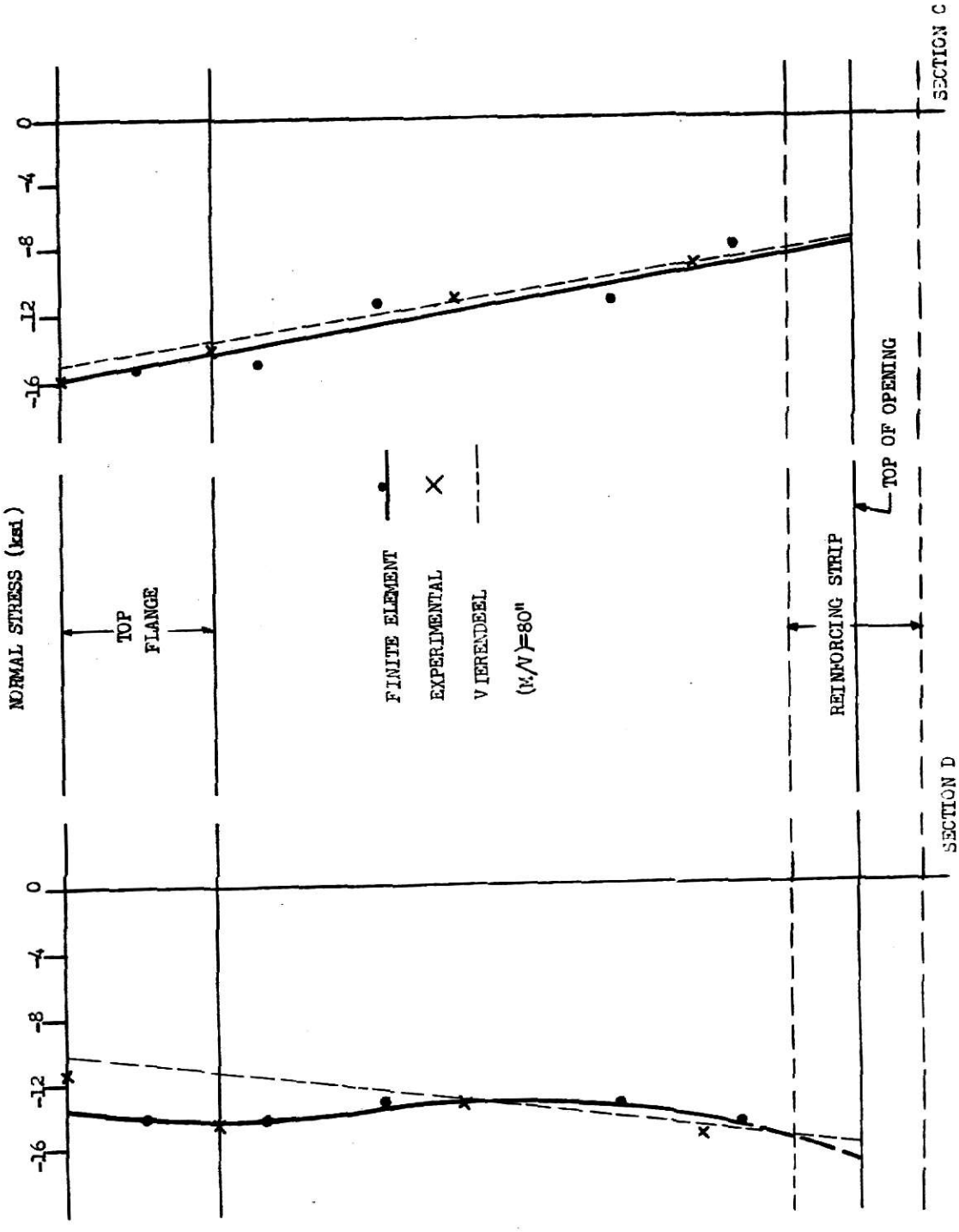

Fig. 23 Normal Stresses For Beam With Reinforcing Strips

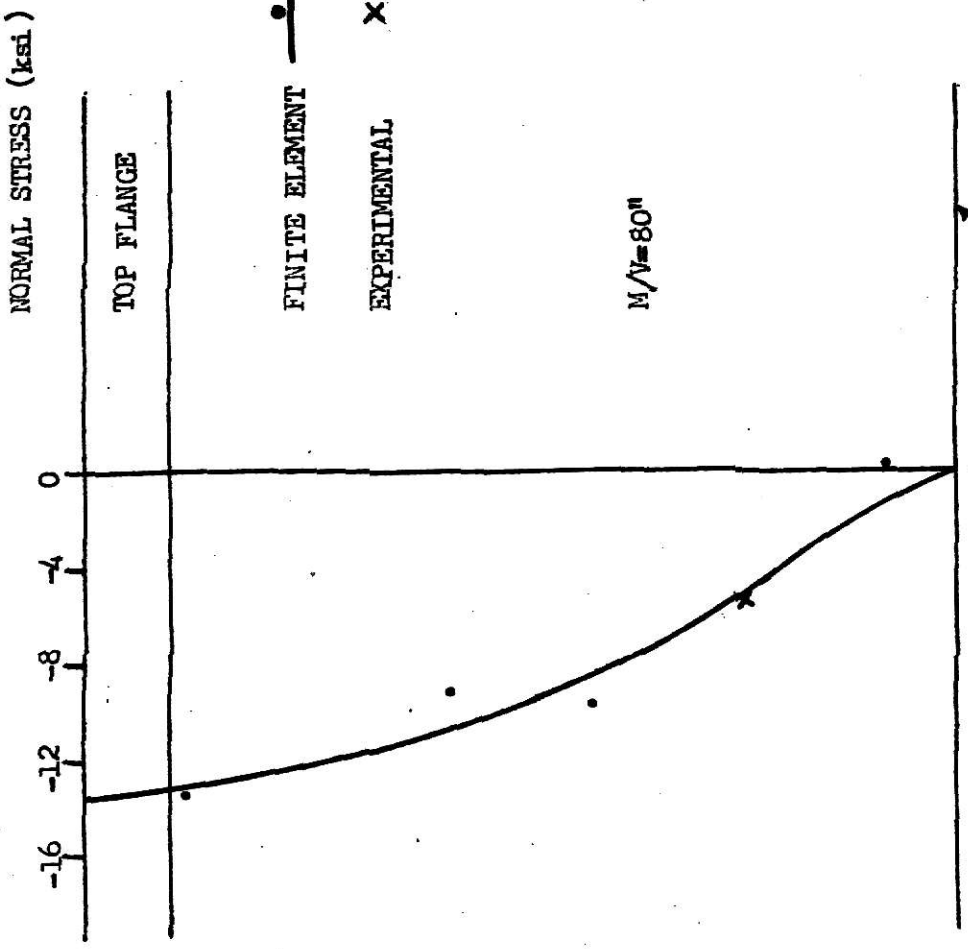

Fig. 24 Normal Stresses For Beam With Reinforcing Strips

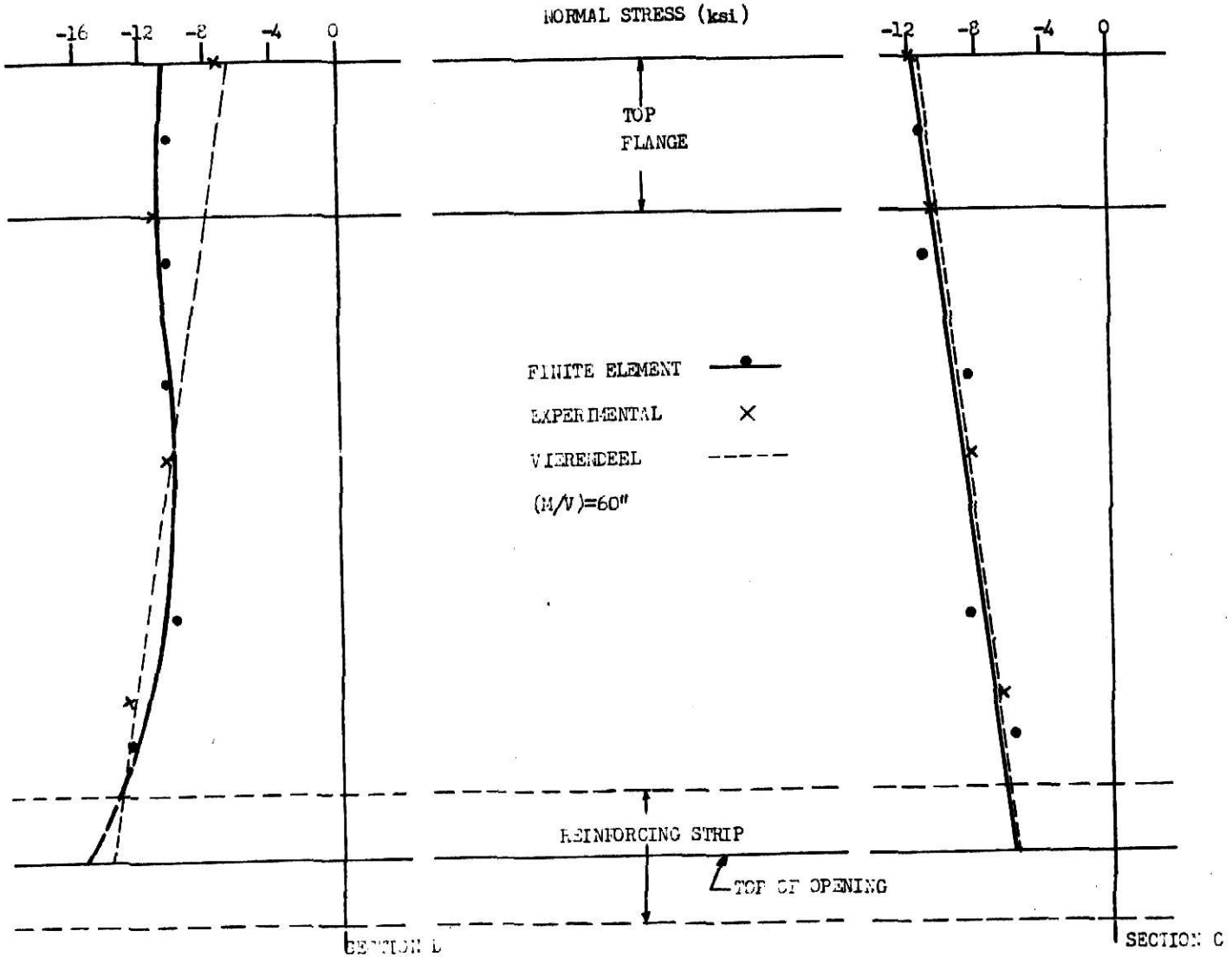

Fig. 25 Normal Stresses For Beam With Reinforcing Strips

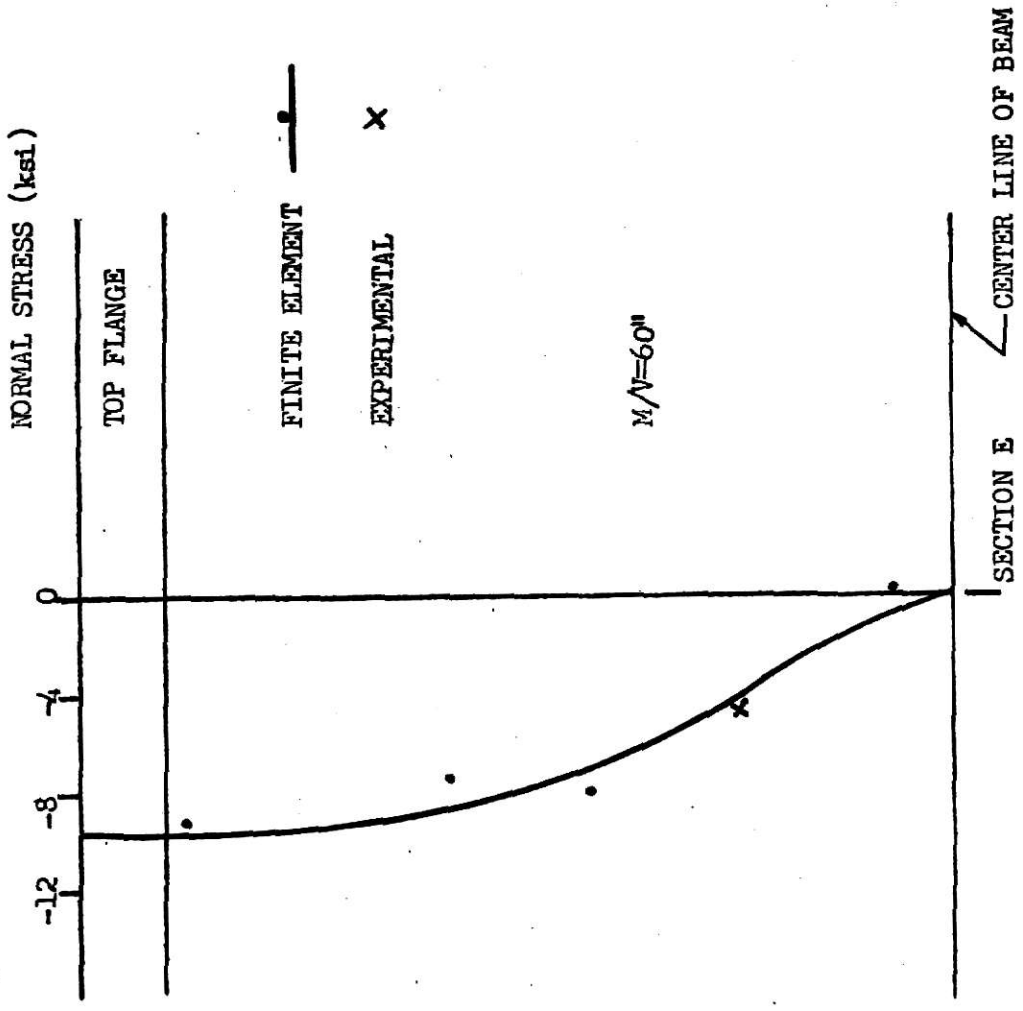

Fig. 26 Normal Stresses For Beam With Reinforcing Strips

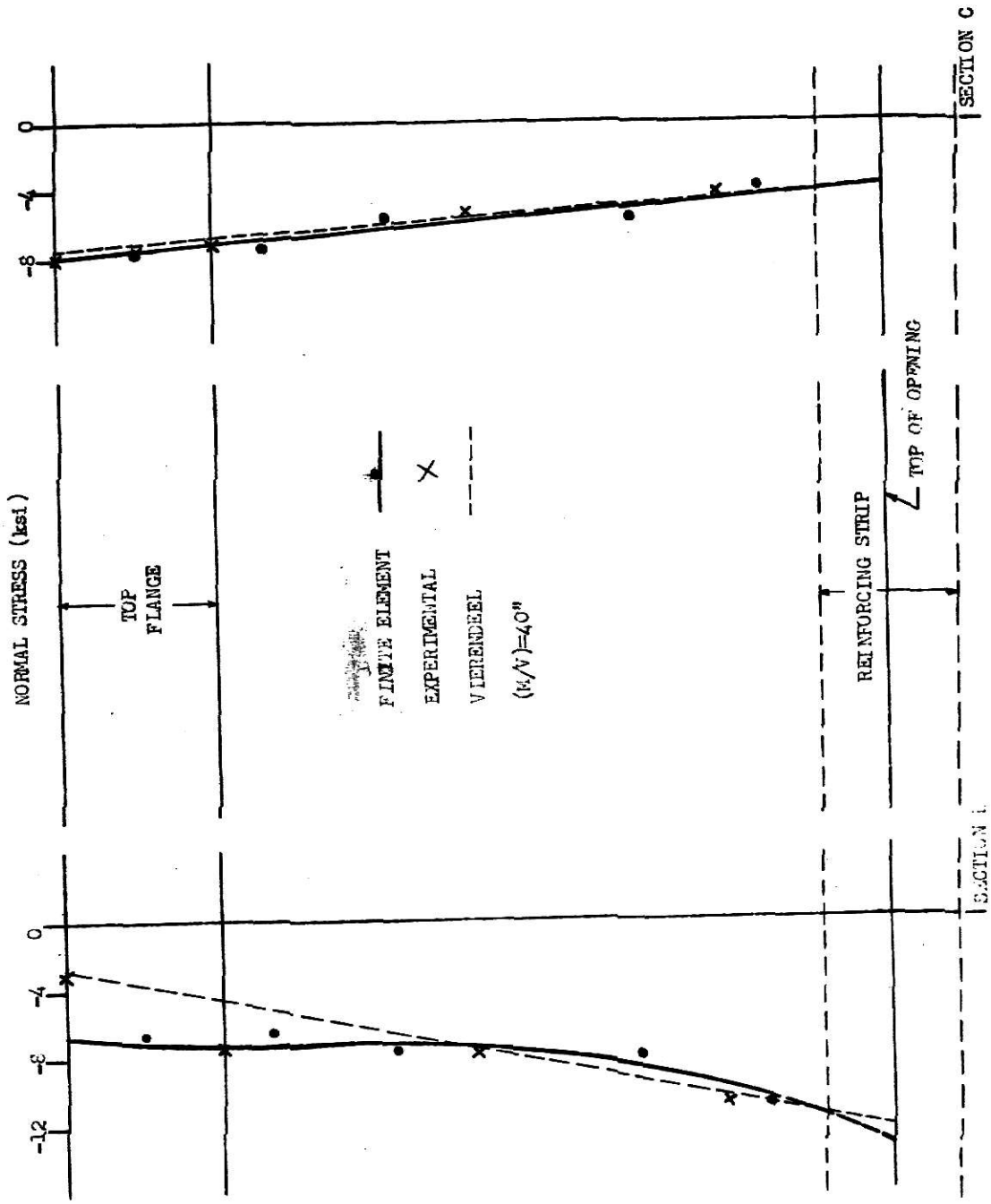

Fig. 27 Normal Stresses For Beam With Reinforcing Strips

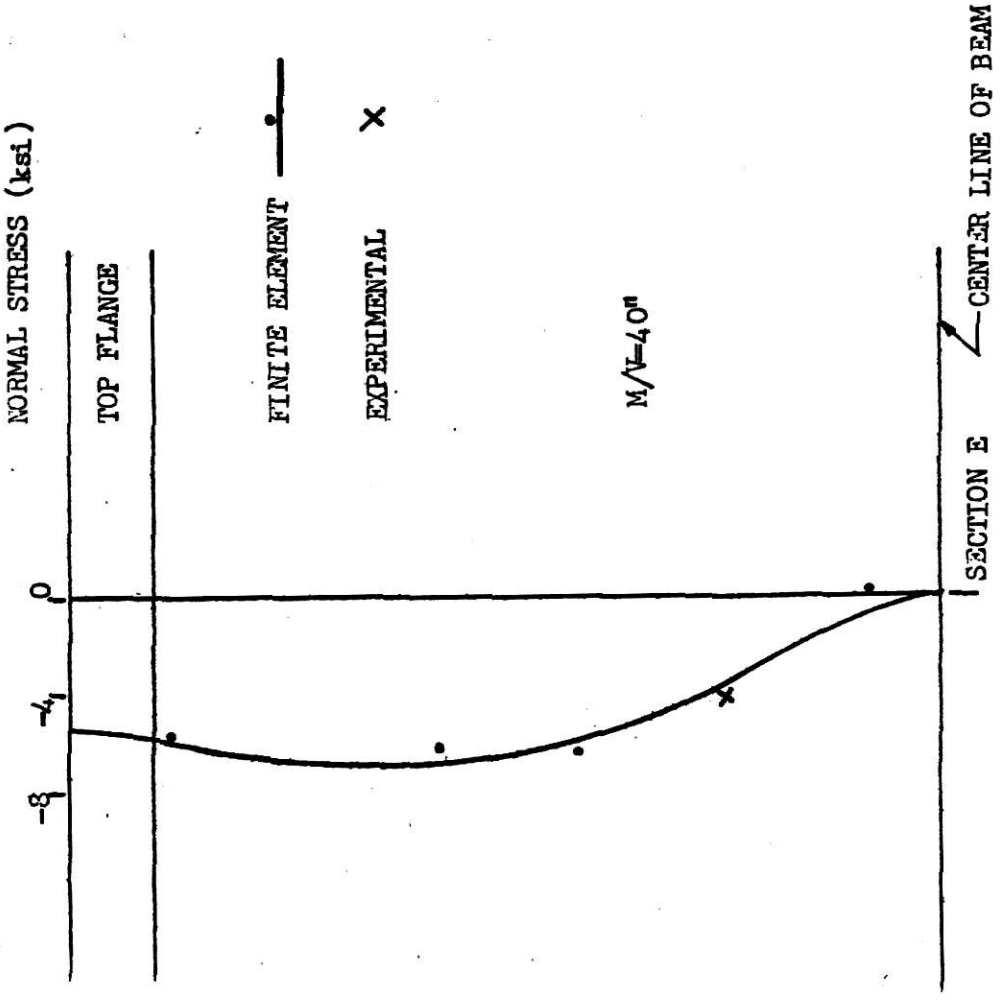

Fig. 28 Normal Stresses For Beam With Reinforcing Strips

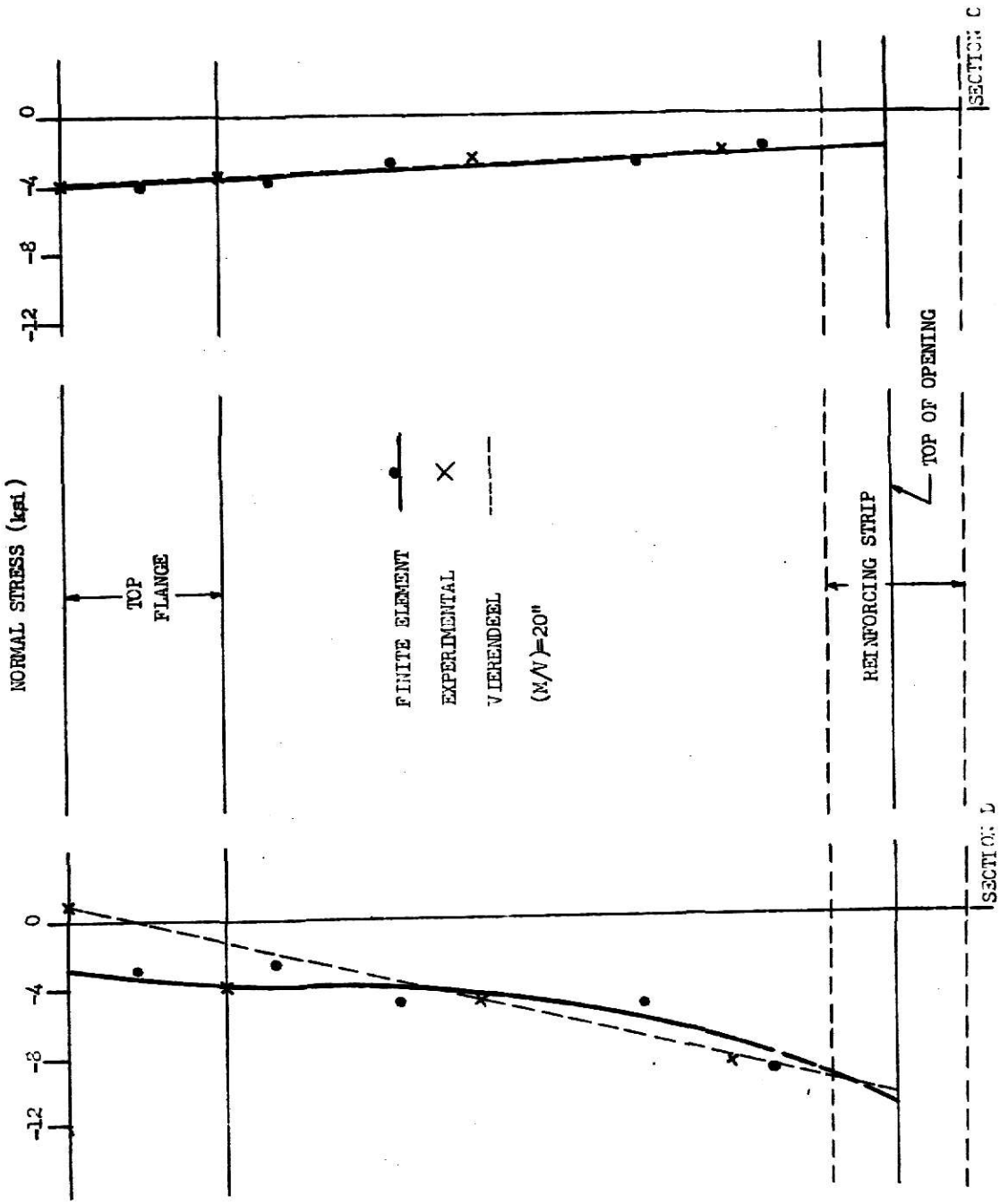

Fig. 29 Normal Stresses For Beam With Reinforcing Strips

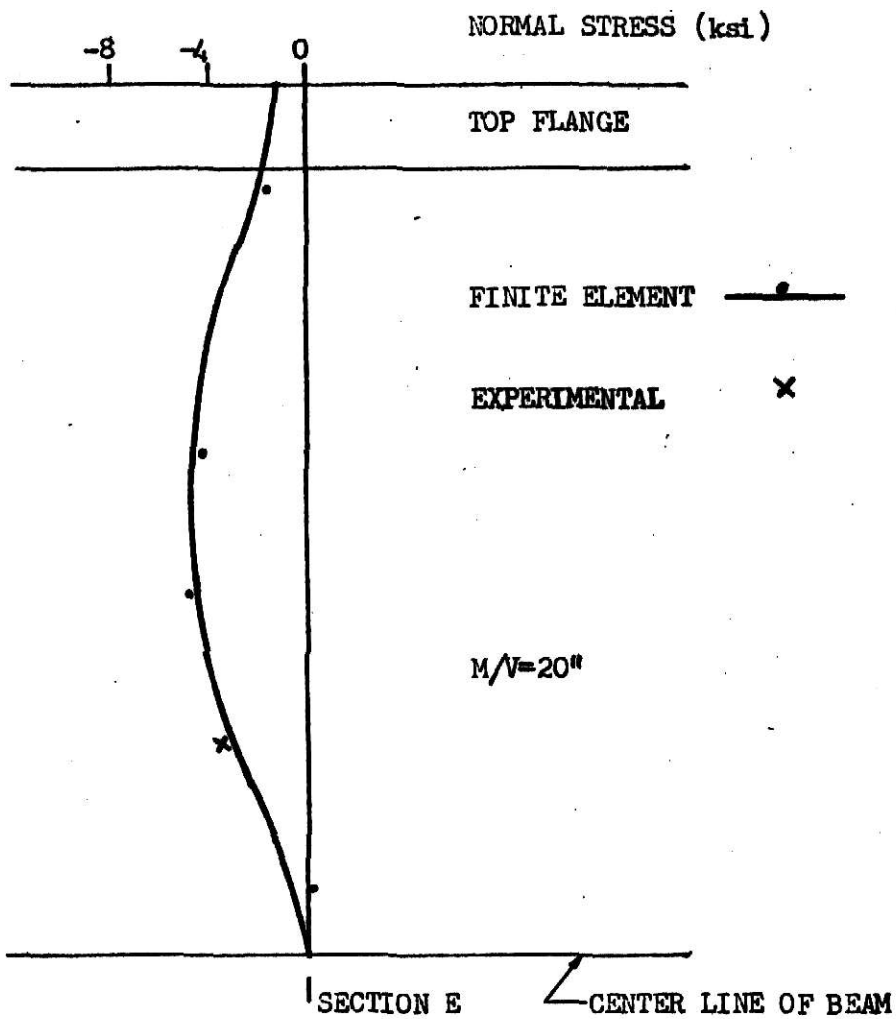

Fig. 30 Normal Stresses For Beam With Reinforcing Strips

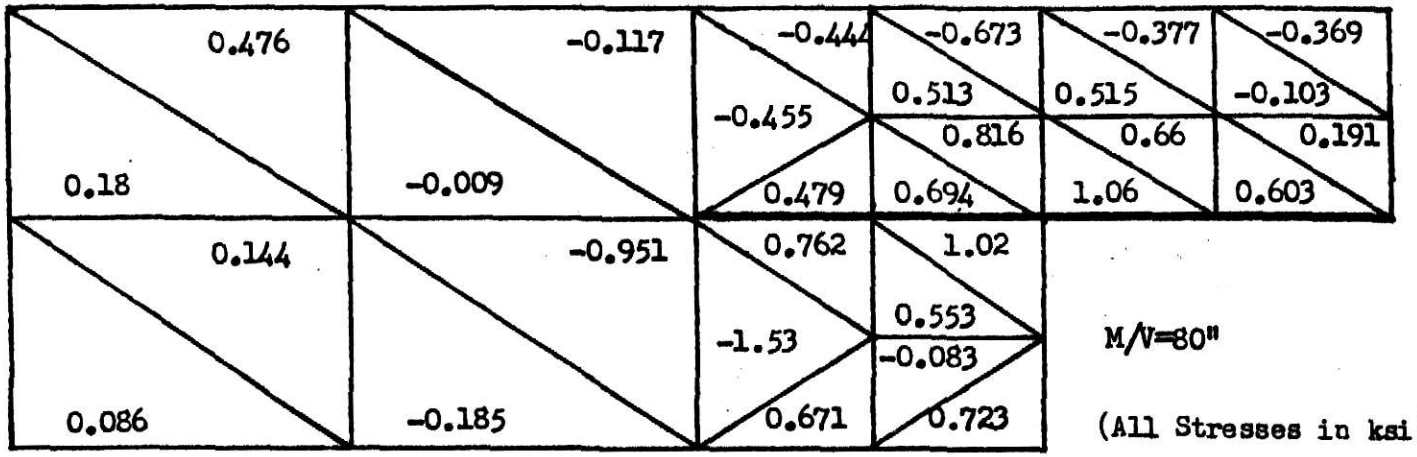

(a) Bending Stresses On The Near Face Of The Plate

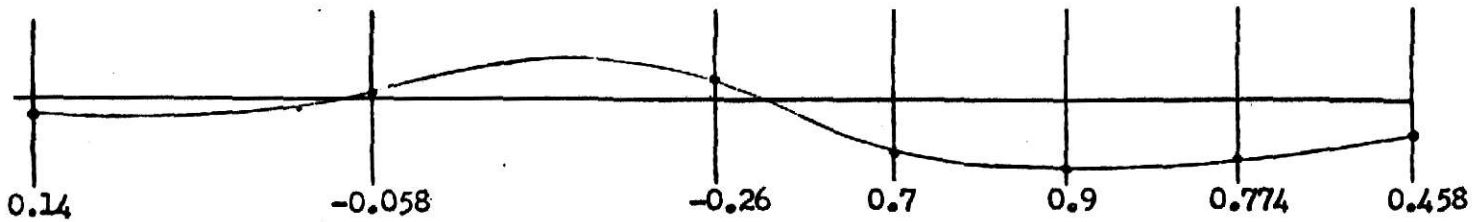

(b) Average Bending Stresses For The Web Along The Line Of The Reinforcing

Fig.31 Bending Stresses For Beam With Reinforcing On One Side Of The Web

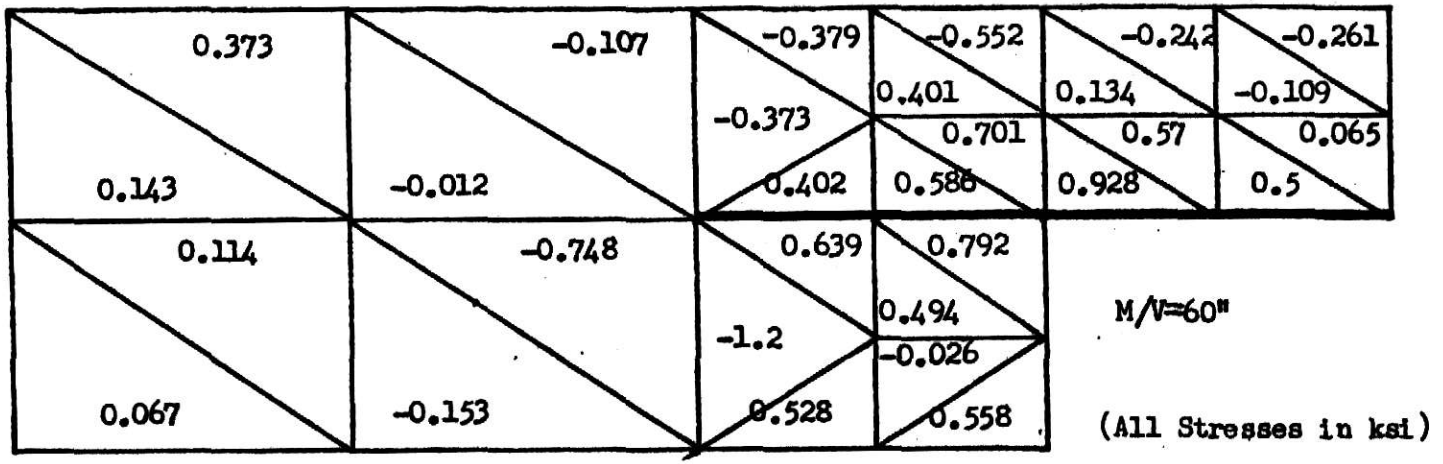

(a) Bending Stresses On The Near Face Of The Plate

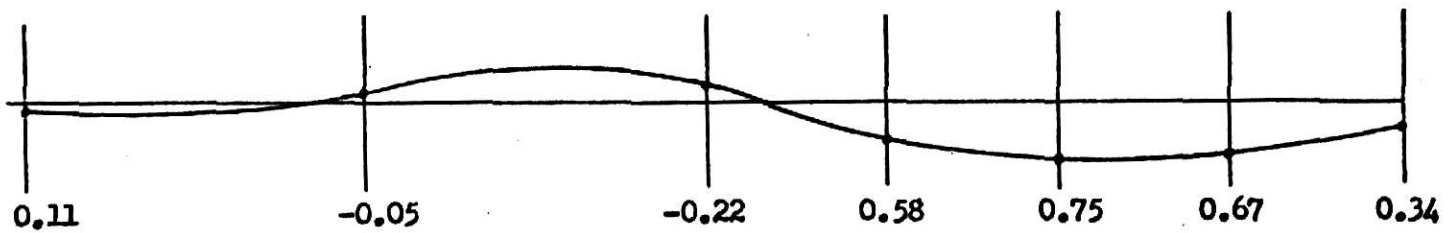

(b) Average Bending Stresses For The Web Along The Line Of The Reinforcing

Fig.32 Bending Stresses For Beam With Reinforcing On One Side Of The Web

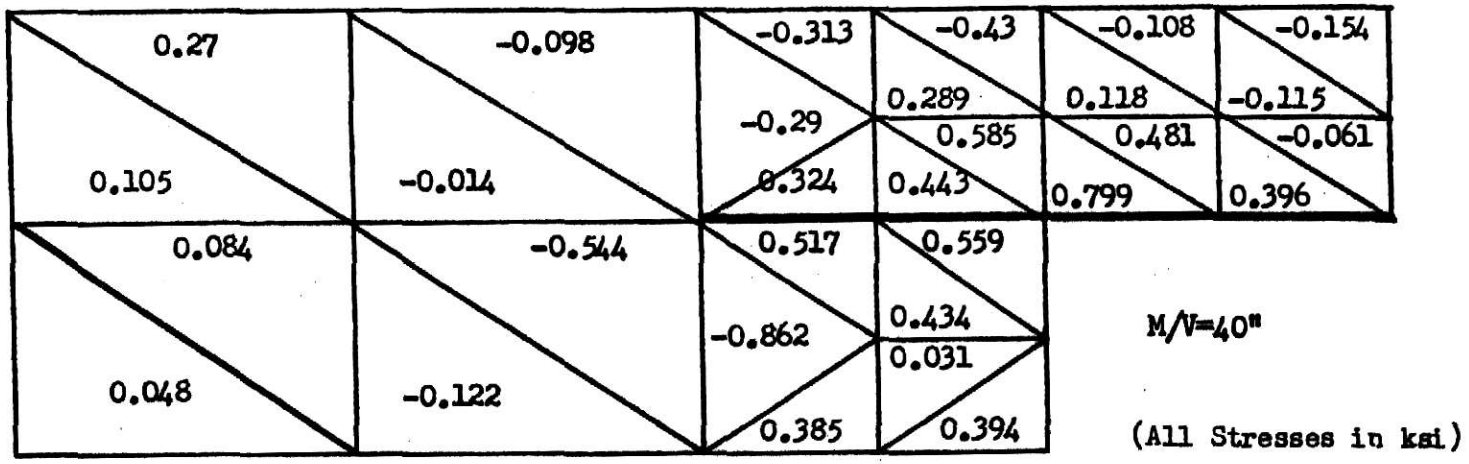

(a) Bending Stresses On The Near Face Of The Plate

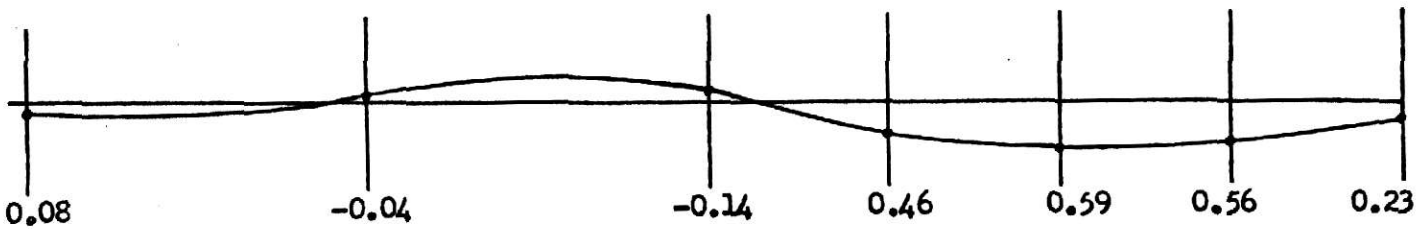

(b) Average Bending Stresses For The Web Along The Line Of The Reinforcing

Fig. 33 Bending Stresses For Beam With Reinforcing On One Side Of The Web

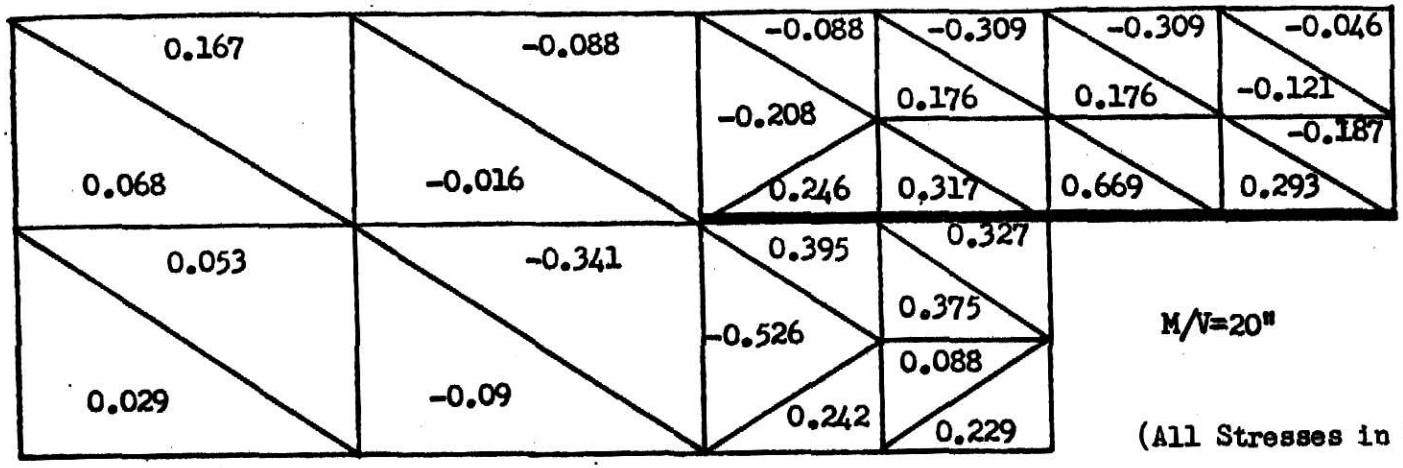

(a) Bending Stresses On The Near Face Of The Plate

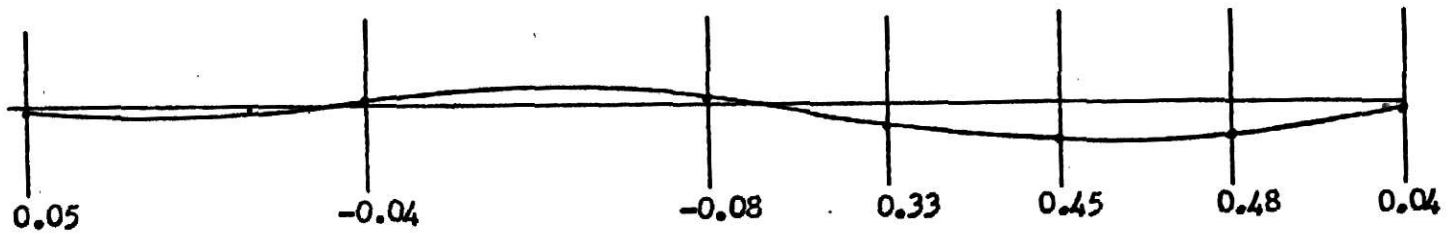

(b) Average Bending Stresses For The Web Along The Line Of The Reinforcing

Fig.34 Bending Stresses For Beam With Reinforcing On One Side Of The Web

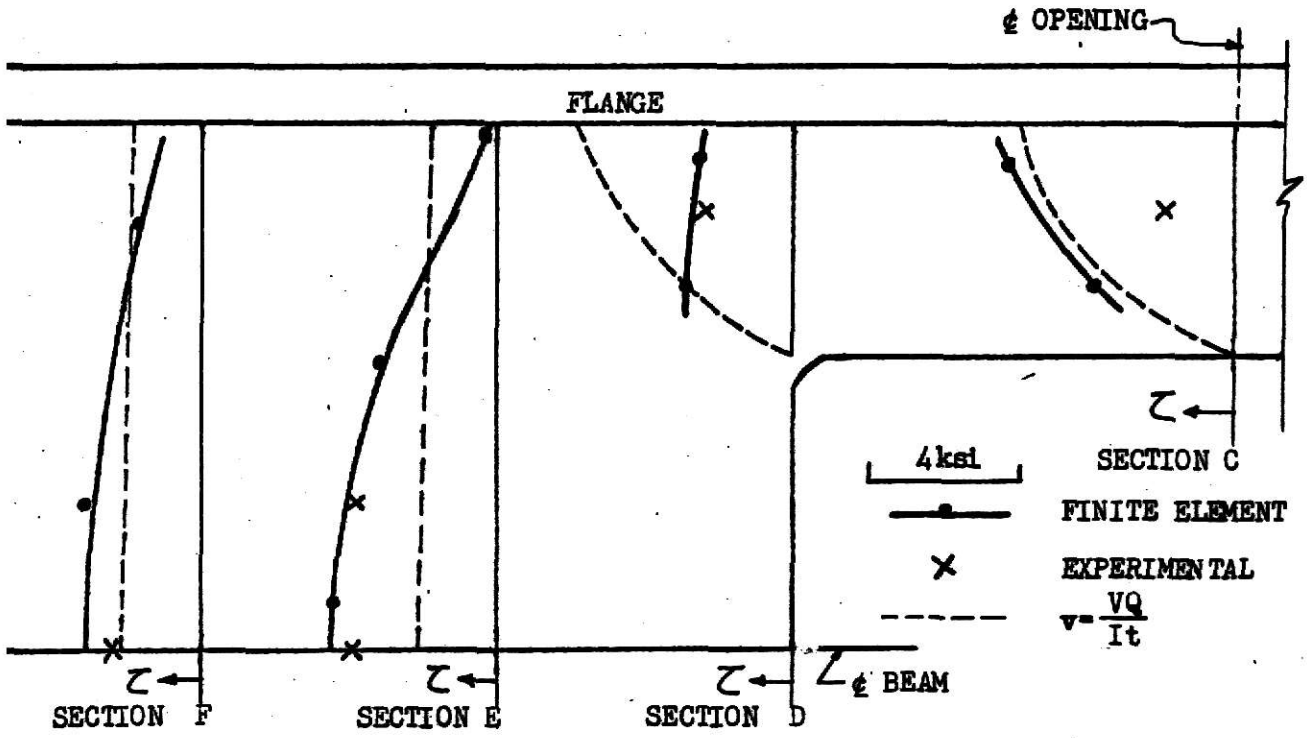

a. Shear Stresses for Beam Without Reinforcing

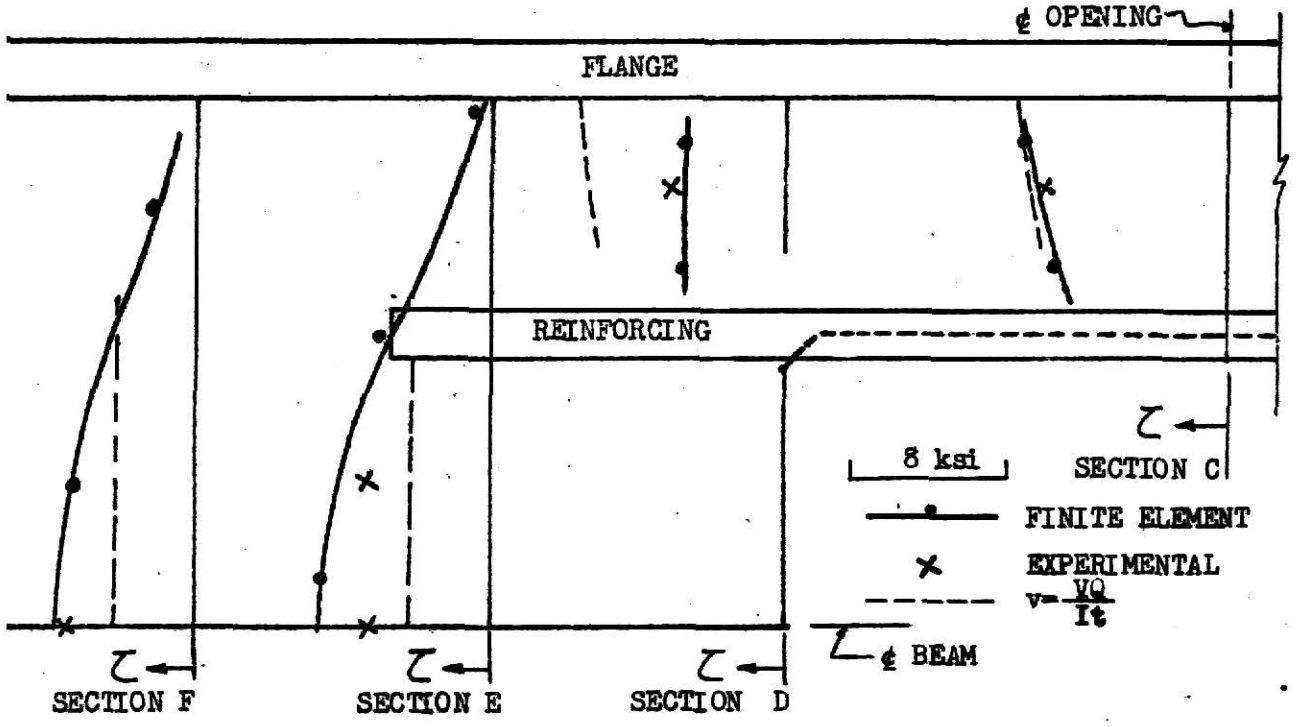

b. Shear Stresses for Beam With Reinforcing

Fig. 35 Shear Stresses

ACKNOWLEDGEMENTS

The auther wishes to express his most sincere appreciation and gratitude to his advisor, Dr. Robert R. Snell, for his valuable guidance and instruction in preparing this report and for reviewing the preliminary manuscript.

Thanks are also due to Dr. Jack B. Blackburn, Head of the Civil Engineering Department, Dr. Peter B. Cooper and Dr. Teddy O. Hodges, members of the advisory committee.

LIST OF REFERENCES

1. Cooper, P. B. and Snell, R. R., "Test on Beams with Reinforced Web Openings," Journal of the Structural Division, ASCE, Vol. 98, No. ST3, March, 1972.
2. Mehrotra, B. L., Mufti, A.A. and Redwood, R. G., "A Program for the Analysis of Three Dimensional Plate Structures," Structural Mechanics Series, No. 5, 1968, Department of Civil Engineering and Applied Mechanics, McGill Univ., Montreal, Canada.
3. Muskhelishvili, N. I., "Some Basic Problems of the Mathematical Theory of Elasticity," 2nd Edition, P. Noorhoff, Ltd., Croningen, The Netherlands, 1963.
4. Heller, Brock and Bart, "The Stresses around a Rectangular Opening with Rounded Corners in a Uniformly Loaded Plate," Proc., 3th National Congress of Applied Mechanics, 1958.
5. Heller, Brock and Bart, "The Stresses around a Rectangular Opening with Rounded Corners in a Beam Subjected to Bending and Shear," Proc., 4th National Congress of Applied Mechanics, 1962.
6. Snell, R. R.,"A Study of the Effect of Reinforcing Configurations for Rectangular Openings in Plates Subjected to Uniaxial Tension," Thesis presented to Purdue Univ., at Lafayette, Ind, in 1963, in partial fulfilment of the requirements for the degree of Doctor of Philosophy.
7. Segner, E. P., Jr,. "Reinforcement Requirements for Girder Web Openings," Journal of the Structural Division, ASCE, Vol. 90, No. ST3, June, 1964.

8. Bower, J. E., "Elastic Stresses around Web Holes in Wide-Flange Beams," Journal of the Structural Division, ASCE, Vol. 92, No. ST2, April, 1966.

9. Bower, J. E., "Experimental Stresses in Wide-Flange Beams with Holes," Journal of the Structural Division, ASCE, Vol. 92, No. ST5, Oct., 1966.

10. Chang, Kho Shu, "Experimental Study of Beam with Web Opening," M. S. Thesis, Kansas State University, 1969.

11. Turner, M. J., Clough, R. W., Martin, H. C., and Topp, L. J., "Stiffness and Deflection Analysis of Complex Structures," Journal of Aeronautical Science, 23, No. 9, 1956.

12. Zienkiewicz, O. C. and Cheng, Y. K., "The Finite Element Method in Structural and Continuum Mechanics," McGraw-Hill Publishing Company Limited, Berkshire, England, 1967.

13. Martin, H. C., "Introduction to Matrix Methods of Structural Analysis," McGraw-Hill Book Company, 1966.

14. Timoshenko, S. P. and Goodier, J. N., "Theory of Elasticity," 3rd Edition, McGraw-Hill Book Company, 1970.

15. Langhaar, H. L.,"Energy Method in Applied Mechanics," John Wiley and Sons, Inc. N. Y., 1962.

16. Timoshenko, S. P., "Theory of Plate and Shells," 1st Edition, McGraw-Hill Book Company, 1940.

PLATE BENDING FINITE ELEMENT ANALYSIS OF BEAMS WITH WEB OPENINGS

by

HSIANG-HUAN LEE

Diploma, Taipei Institute of Technology,
Taiwan, China, 1965

AN ABSTRACT OF A MASTER'S REPORT

submitted in partial fulfillment of the

requirements for the degree

MASTER OF SCIENCE

Department of Civil Engineering

KANSAS STATE UNIVERSITY
Manhattan, Kansas

1972

ABSTRACT

The purpose of this investigation was to obtain the results of an analytical solution for the problem of a beam with a rectangular web opening based on a finite element method and to compare these results with those of an experimental program carried out at Kansas State University. The results were also compared with the results obtained using a Vierendeel Analysis.

An A36 W12x45 Steel beam with a 6" x 9" rectangular web opening at middepth, subjected to combined bending and shear with four different moment-shear ratios was treated as a three dimensional plate structure in this study. The beam without reinforcing was studied first and then two longitudinal reinforcing strips were placed on one side of the web, above and below the opening.

The results based on the finite element analysis indicated good agreement with the experimental data and provided a more reasonable stress distribution than the so-called 'Vierendeel Analysis' away from the center of the opening. Furthermore, the use of one-sided reinforcing strips had little effect on the stress distribution since the bending stresses induced in the web were relatively small compared with the normal stresses.